frontiers | Frontiers in Energy Research

TYPE Original Research
PUBLISHED 01 February 2024
DOI 10.3389/fenrg.2024.1348458

OPEN ACCESS

EDITED BY
Muhammad Farooq,
University of Engineering and Technology, Pakistan

REVIEWED BY
Haroon Farooq,
University of Engineering and Technology, Pakistan
Ishak Ertugrul,
Mus Alparslan University, Türkiye
Rami Reddy,
Chonnam National University, Republic of Korea

*CORRESPONDENCE
Abdullah Altamimi,
a.altmimi@mu.edu.sa
Zafar A. Khan,
zafarakhan@ieee.org

RECEIVED 02 December 2023
ACCEPTED 04 January 2024
PUBLISHED 01 February 2024

CITATION
Mujahid K, Altamimi A, Kazmi SAA, Khan ZA, Alharbi B, Alafnan H, Alshehry H and Mir AA (2024), An intelligent multi-layer, multi-agent MMG framework with amelioration of energy efficiency and future investment outlook, under the deregulated day-ahead and real-time market regime.
Front. Energy Res. 12:1348458.
doi: 10.3389/fenrg.2024.1348458

An intelligent multi-layer, multi-agent MMG framework with amelioration of energy efficiency and future investment outlook, under the deregulated day-ahead and real-time market regime

Kamran Mujahid[1], Abdullah Altamimi[2,3]*, Syed Ali Abbas Kazmi[1], Zafar A. Khan[4,5]*, Bader Alharbi[2], Hamoud Alafnan[6], Halemah Alshehry[2] and Aneeque A. Mir[7]

[1]U.S.-Pakistan Center for Advanced Studies in Energy (USPCAS-E), National University of Sciences and Technology (NUST), Islamabad, Pakistan, [2]Department of Electrical Engineering, College of Engineering, Majmaah University, Al-Majmaah, Saudi Arabia, [3]Engineering and Applied Science Research Center, Majmaah University, Riyadh, Saudi Arabia, [4]School of Computing and Engineering, University of Huddersfield, Huddersfield, United Kingdom, [5]Department of Electrical Engineering, Mirpur University of Science and Technology, Mirpur, Pakistan, [6]Department of Electrical Engineering, College of Engineering, University of Ha'il, Ha'il, Saudi Arabia, [7]Department of Engineering Sciences, University of Oxford, Oxford, United Kingdom

This paper developed an intelligent multi-agent system (MAS) with a multi-layer framework for multi-microgrids (MMGs) using robust and modern communication patterns for deployed agents to achieve distributed tasks. The MMG paradigm introduces three microgrids (MGs) based on the type of load, working environment, and living habitat: residential, commercial, and industrial. In addition, a day-ahead and real-time model is proposed for day-ahead and real-time signals. Intelligent agents in the multi-layer MAS framework make smart decisions based on multiple algorithms to optimize schedule power and minimize costs, considering demand dispatch and demand response as core components. Maximum renewable energy utilization aims to increase user comfort and reduce greenhouse gas (GHG) emissions. Load agents deployed in each MG ensure maximum efficiency. The proposed framework recommends various tariff rates and tariff adjustment strategies to promote and offer an economic evaluation across the respective indices. To minimize the monopoly of the energy market, an efficient energy market model is developed for the proposed MMG paradigm to maximize the competition by incorporating future and spot-market trading schemes for day-ahead and real-

Abbreviations: MM, modified multi-objective; DD, demand dispatch; DR, demand response; MAS, multi-agent system; L, M, and S: large, medium, and small; SRMG, smart residential microgrid; SCMG, smart commercial microgrid; SIMG, smart industrial microgrid; R, M, and P: rich, middle, and poor; P_{sur}, surplus power; γ_0^1, device status; 1 = ON; 0 = OFF; η_{RTE}, round-trip-efficiency of the BESS; EEMMC, efficient energy management market controller; DAM, day-ahead model; RTM, real-time model; $TL_{devices}$, total load of devices; MMPPnP, modified multi-objective-prioritized plug-and-play; GWO, gray wolf optimization.

time signals. The comparative analysis indicates optimized results based upon the cost-benefit analysis, cost reduction, power transaction in the market, and maximum utilization of renewable energy resources (RERs).

KEYWORDS

multi-agent systems, multi-microgrid, energy management, day-ahead, real time, intelligent agent multi-agent systems, intelligent agents

1 Introduction

1.1 Background

According to the International Energy Agency, the renewable energy utilization rate increased by 3.7% in 2019, a minor increase compared to that of the previous year. Wind (150 TWh) and solar (140 TWh) power accounted for 27% of the global electricity supply and contributed to 85% of renewable energy growth. The main factors contributing to such growth are extensive support in policy and a reduction in technological prices. Consequently, the power sector lowered greenhouse gas (GHG) emissions by nearly 170 Mt in 2019 (IEA, 2020). Furthermore, in a microgrid, to tackle the resiliency and reliability issues arising from the intermittent nature of renewable energy resources (RERs), this concept has been introduced to maximize energy utilization and the power system's credibility. According to the U.S. Department of Energy, a microgrid (MG) is a group of interconnected loads and distributed generation resources (DERs) within clearly defined electrical boundaries that act as a single controllable entity concerning the grid (Ton and Smith, 2012).

The microgrid's broader concept revolves around the deployment of self-sufficient distributed electricity generation resources on a small scale along with the energy storage systems (ESSs) near the consumers with adequate controllability over consumption demand (Hirsch et al., 2018). The generation resources may also include conventional resources along with clean energy. Microgrids can operate in two modes: grid-connected and islanded. The decentralized and distributed architecture of the resources in microgrids completely negates the transmission losses. Microgrid ecosystems allow automation, controllability, and monitoring of distributed assets within a cost-effective economic operation, making them less expensive than centralized and main-grid systems (Cortes et al., 2017). Multi-microgrids (MMGs) can be referred to as a networked cluster of adjoining microgrids for coordination of energy management and interactive assistance among each other (Xu et al., 2018).

The interconnectivity of microgrids uses different factors, including the more effective use of renewable energy sources, lower operating costs, black-out support, increased stability, and resiliency (Alam et al., 2020). All the benefits mentioned above are achievable through effective energy management in both the microgrid and multi-microgrid paradigms. Energy management is widely applicable to achieve optimal load scheduling based on available energy and market considerations. Energy interactions across the grids under the multi-microgrid paradigm boost stakeholder engagement, resulting in more competitive energy markets. As a result, the MMGs' power and economic stability have improved (Yang et al., 2019). According to Khalid et al. (2019), energy management improves grid dependability and stability while lowering customer costs and usage. Zlatkovic et al. (2019) applied demand side management using real-time pricing and an inclining block rate (IBR) tariff to schedule a load for homes effectively.

Demand side management (DSM) is a method of energy management that benefits both customers and utilities. Liang et al. (2019) implemented the demand response on a commercial building to achieve satisfactory user comfort within an optimal operating cost range. Demand response is one of the techniques of demand side management, which allows users to change their consumption patterns at peak hours in response to the pricing signal. In addition to residential and commercial MGs, industrial microgrids have also gained popularity in recent years. Naderi et al. (2017) shows the planning of industrial estate for maximizing renewable resource utilization, keeping in view the reliable and sustainable operation of sensitive loads. Choobineh and Mohagheghi (2016) proposed a framework for the industrial microgrid that can achieve optimal energy usage, reduce the cost, and delay the lifetime of assets. The number of MGs in distribution networks has increased dramatically due to the fast adoption of DERs. As a result, MG interaction and energy exchange are significant concerns in multi-microgrid systems.

Tan and Chen (2020) aimed to concurrently minimize the system's cost, emissions, and loss through multi-objective optimization. Ahmadi and Rezaei (2020) decreased the cost and increased the generation performance of the multi-microgrid framework using the proposed the demand response program (DRP) strategy in energy management. To deploy a microgrid, it is necessary to undertake an economic study of the project, allowing investors to relate to it. Husein and Chung (2018) conducted an economic analysis for designing an optimal microgrid considering the tax benefits and incentives of integrating RERs. Oueid (2019) discussed the financial information required for planning MGs to facilitate evaluating similar projects. The Microgrid Decision Support Tool (MDSTool) was used in Vu et al. (2019) to conduct a detailed technical and economic analysis of grid-connected PVs with the energy storage system to achieve an optimal university microgrid. The net present value (NPV) is used as a metric for economic evaluation of the project. The MMG system's dependability and economic evaluations are studied in Wang et al. (2018).

1.2 Literature review and research gap

In multi-microgrids, an energy management system (EMS) is used to optimize the scheduling of power resources and energy

TABLE 1 Modeling details of the complete MMG setup.

Base load of SRMG appliances	LED bulb	Ceiling fan	Wi-Fi router	LED TV	Coffee maker	Laptop
Power (W)	50	50	6	80	1,317	60
Category (rich (R), middle (M), and poor (P))	R/M/P	R/M/P	R/M/P	R/M/P	R	R/M/P

PFDs and TFDs of SRMGs					
Appliance	Power (W)	Category (R, M, and P)	Appliance	Power (W)	Category (R, M, and P)
VAC	2,500–4,500	R	Washing machine	730	R/M/P
AC	1,400–1,800	R/M	Dishwasher	1,000	R/M/P
Refrigerator	500	R/M/P	Microwave oven	500	R/M/P
Ironing machine	1,000	R/M/P	Clothes dryer	2,000	R
Cooler	40	P	Water pump	746	R/M/P
Base load of SCMG appliances	Power (W)	Category (L, M, and S)	Appliance	Power (W)	Category (L, M, and S)
Syringe pump	20	L	Telecommunication tower	5,000	L/M/S
Mechanical ventilator	38	L	ATM machine	75	L/M
Patient monitors	35	L	Elevator	3,400	L/M
Blood pressure cuffs	5	L	Ceiling fan	80	L/M/S
Centrifugal device	180	L	Laser printer	450	L/M/S
LED bulb	13	L/M/S	Angiography	9,000	L
Desktop computer	180	L/M/S	MRI	13,000	L
Laptop	60	L/M	CT scanner	5,000	L/M
Ice cream Machine	1,800	L/M/S	Radiography	1,400	L/M/S
Medium-duty commercial microwave	1,500	L/M	Ultrasound	800	L
Biochemistry analyzer	65	L/M	Treadmill	1,679	L
Oxygen concentrator	480	L/M/S			

(Continued on following page)

10.3389/fenrg.2024.1348458

TABLE 1 (*Continued*) Modeling details of the complete MMG setup.

Base load of SRMG appliances	LED bulb	Ceiling fan	Wi-Fi router	LED TV	Coffee maker	Laptop

PFDs and TFDs of SCMGs					
Appliance	Power (W)	Category (L, M, and S)	Appliance	Power (W)	Category (L, M, and S)
HVAC	2,500–4,500	L/M/S	MRI	13,000	L
C/deep freezer	450	L/M/S	CT scanner	5,000	L/M
Commercial REF	500	L/M/S	Ultrasound	800	L
Vending machine	183	L/M	Biochemistry analyzer	65	L/M
AC	1,400–1,800	L/M	Agriculture tubewell	5,000	L/M/S
Clothes dryer	3,000	L/M/S	Water pump	8,000	L/M/S
Radiography	1,400	L/M/S	Commercial W/machine	1,000	L/M/S
Commercial Iron	2,200	L/M/S	Commercial cooler	200	S

Base load of SIMGs		
Appliance	Desktop computer	GreenUp High-bay BY550 lights
Power (W)	180	200

TFDs and PFDs of SIMGs			
Appliance	Power (kW)	Appliance	Power (kW)
Crusher	130	Clinker cooler	15
Conveyor belts	50	Cement mill	68.25–78.75
Bucket elevator	4	Conveyor belts	50
Vertical roller mill	67.5–87.5	Packaging	25.5
Bucket elevator	4	Washing of olives	9.06
Gravity-type blending	0.13	Crusher	22.4
Rotatory kiln	760–840	Paste production	5.5
Extraction	22	Separation	5.5

10.3389/fenrg.2024.1348458

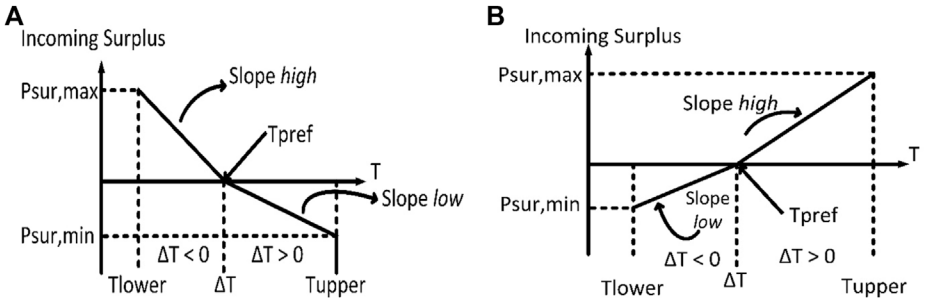

FIGURE 1
Behavior of intelligent thermostats for a **(A)** cooling system and **(B)** heating system.

storage devices to ensure supply–demand equilibrium through exchanging power among grids by adopting different trading mechanisms. During the last few years, there has been a surge of attention on the EMS among researchers for interconnected multi-microgrids. A hierarchical Stackelberg game model in an MAS with three separate stack-holders was proposed in Dong et al. (2020). The suggested energy trading model maximizes each participant's economic rewards while achieving energy management via the incentive demand response. However, existing research does not include a full sensitivity analysis of this model nor provides detailed information about the load type in microgrids. Furthermore, the model considers only day-ahead operation for all the three stack-holders and ignores real-time operation. Within the multi-microgrid paradigm, Zhuo et al. (2019) suggested an independent MG for battery energy storage systems (BESSs). Parallel to demand response initiatives, the independent BESS will maximize the share of renewable energy sources while reducing grid power dependency. However, the studies cannot provide a detailed study of the suggested framework's financial report and scheduled load. Bui et al. (2018) proposed the concept of adjustable power in a multi-agent framework for a multi-microgrid paradigm. Mixed-integer linear programming (MILP) underpins all established models, making them simple to apply and computationally inexpensive. The proposed methodology reduces the MMG's operational costs while ignoring GHG emissions.

Using model predictive control (MPC) and two-stage stochastic programming with recourse, Systems et al. (2020) proposed an efficient control technique for a hierarchal framework-based MMG system with integrated energy management. The authors claim to have achieved a reduction in grid power exchange as well as an optimal solution technique for power scheduling. Yin and Li (2021) focused on developing an energy management framework for achieving decentralized autonomous microgrids that operate in an MMG system with optimal operation coordination. The hybrid metaheuristic multi-layer reinforcement learning technique is implemented to lower the peak-to-average ratios, reduce power fluctuations, lower operational costs, lower computational strain, and improve load forecasting. By deploying fuzzy-based peer-to-peer energy exchange in interconnected multi-microgrids, the energy management technique presented in Thirugnanam et al. (2021) minimizes the cost of consumer energy use. The random vector functional link network (RVFLN) technique models load demand and distributed generators (DGs). For peer-to-peer energy exchange, dynamic pricing is used. This work does not go through the different loads or how they are scheduled. Additionally, the availability of historical data is a barrier to deploying such models.

A unique online consensus alternating direction method of multipliers (OC-ADMM) algorithm is presented in Guo et al. (2021) to handle P2P trading mechanisms in real-time. This mechanism lessens the computational burden with precise assessment and maximizes online social welfare. The distributed power management system discussed in Rajaei et al. (2020) is based on the alternating direction method of multipliers (ADMM) in the distributed MMG hierarchy for day-ahead operational scheduling considering the technical constraints of the distribution network. Unlike a conventional centralized controller, a transactive energy signal initiates ADMM and MG scheduling processes for distributed microgrid coordination. Liu et al. (2021) optimized energy scheduling and the trading of microgrid and electric vehicles with nearby microgrids by considering the availability of fast charging services in the MAS framework. The authors used convex optimization to solve the problem of time-flexible EV driving. Purage et al. (2022) aimed at achieving market equilibrium, global optimality, and microgrid constraint without invading market participants' privacy in a decentralized P2P energy trading mechanism.

The ADMM is applied to each market participant for coordination in the proposed market framework. Energy management for four nanogrids comprising two residential, one commercial, and one industrial building was presented in Ramadan et al. (2019). The authors viewed nanogrids as prosumers or aggregators, resulting in an effective demand response (DR) and lower operational costs. Using the MATLAB and JADE framework for Multi-Agent Network (MAN) deployment, a hybridized reinforcement learning and powerful machine learning algorithm accomplished optimal trading and scheduling of nanogrids. The authors, however, neglect to specify the load details for each nanogrid. Rezaei et al. (2022) introduced conditional value-at-risk (CVaR) into the scheduling problem of the MMG system to reduce the low-profit risk even in the worst-case situation. The findings show

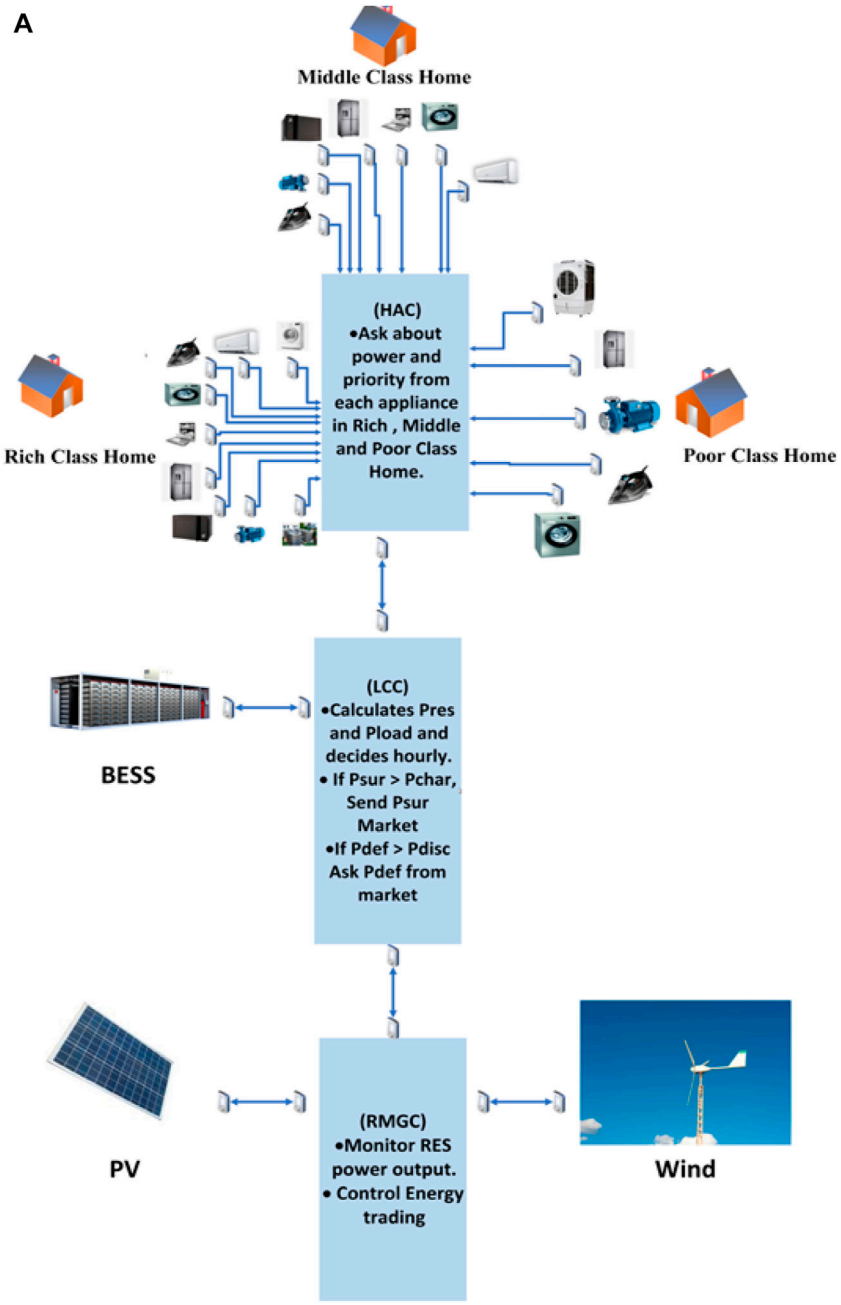

FIGURE 2
(Continued).

that raising the emission factor and risk does not influence the predicted profit decrease. Karimi and Jadid (2023) proposed a tri-layer integrated energy system framework in the MG that minimizes costs and maximizes the integration of RERs. However, the proposed work has not considered the economic analysis and device-level load scheduling. Furthermore, the proposed framework fails to minimize the robustness of an operation at each layer.

Karimi et al. (2023) suggested the Average Power Flexibility during Peak Period Index (APFDPPI) to reduce the occurrence of new peaks and maximize the reliability of the MMG system due to the uncoordinated DR. Real-time (RT) MMG operation and economic evaluation for independent investors are not presented in the proposed research. A bi-layer predictive energy management system (PEMS) is deployed (Xu et al., 2023) in uncertain renewable multi-energy systems for reliable operation of microgrids and to reduce operational costs. The authors have not discussed the energy transaction among grids and the details of the MG load nature and its scheduling. Ali et al. (2023) proposed the energy management system for the residential load only but have neglected the priorities to be assigned to the appliances during low

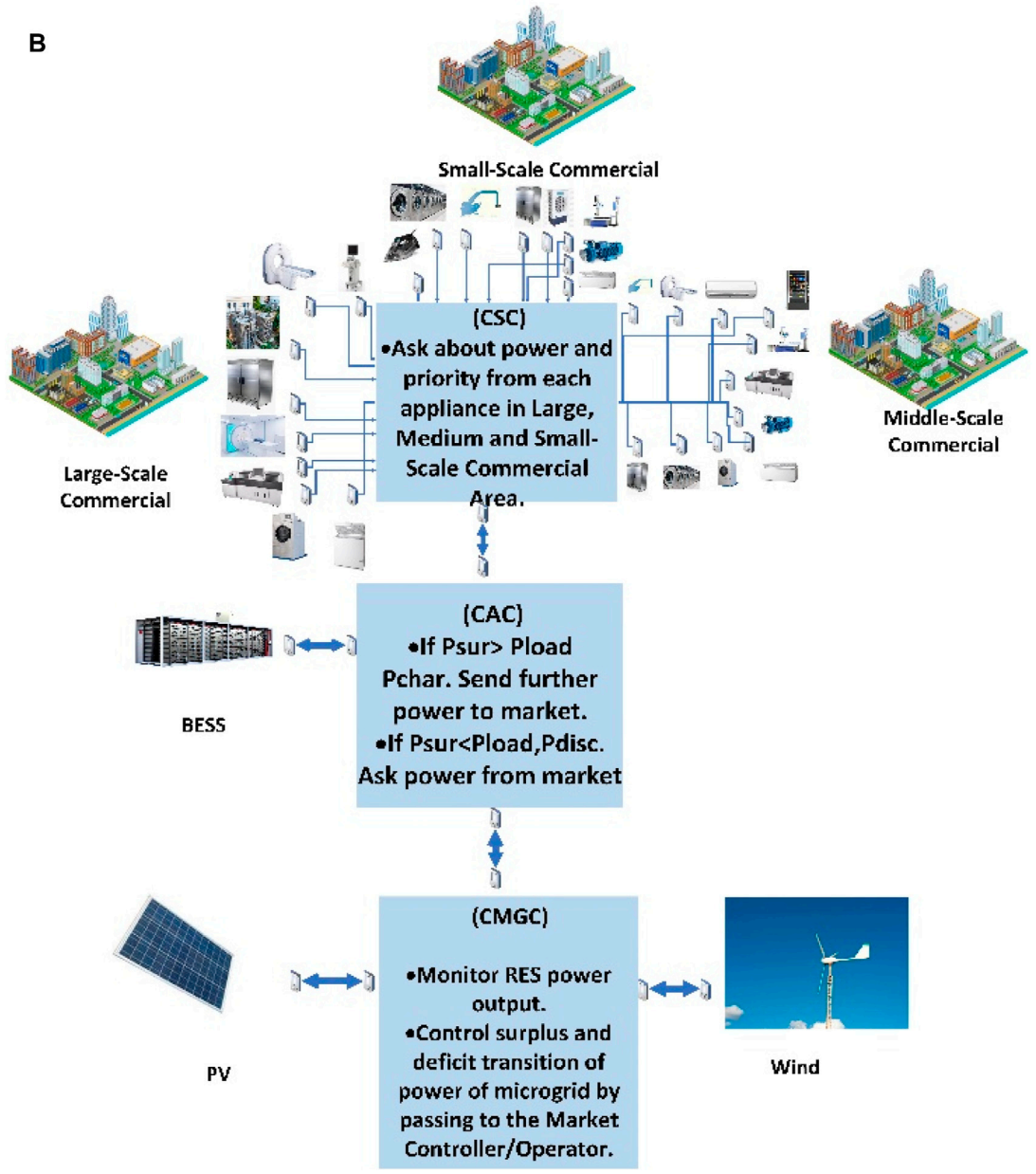

FIGURE 2
(Continued).

generation power. Furthermore, the economic viability of the MG for power transactions in the energy market is not highlighted. To ensure the reliable and stable operation of the MG cluster, a centerless control strategy is employed in Shi et al. (2023). The proposed work has not discussed the energy management strategies for efficient operation of MGs. Furthermore, the techniques to use renewables and load scheduling are also neglected. Zhong et al. (2022) used the ADMM in day-ahead scheduling to reduce the MMG's operating expenses and increase energy while maintaining confidentiality. For each MG, the rolling horizon method is employed for intra-day scheduling to lower the charge and expenses.

1.3 Contributions and organization of the paper

The contribution of the proposed work is two-fold. First, the technical and economic perspectives of the proposed work are covered. This paper's contributions are summarized as follows:

- This paper proposes a cost-effective and energy-efficient solution through energy management modeling of three different load nature multi-layered agent-based hierarchical interconnected and grid-connected microgrids: smart residential microgrid, smart commercial microgrid, and smart industrial microgrid.

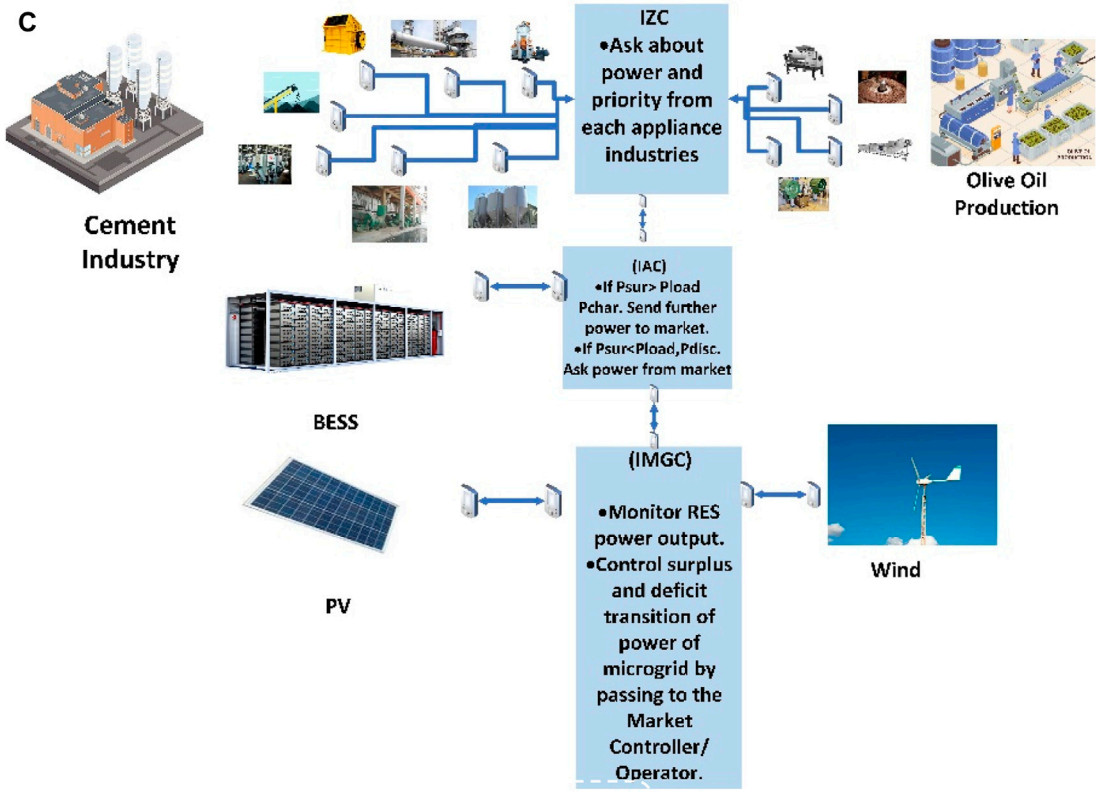

FIGURE 2
(Continued). Illustration of the multi-microgrid setup: **(A)** SRMG; **(B)** SCMG; **(C)** SIMG.

- The proposed scheme provides optimal control over personal comfort, pricing, and bilateral power transactions in energy markets by deploying a robust and secure multi-agent system framework in the Python environment.
- The proposed framework develops a deregulated market for real-time and day-ahead signals by providing spot-market and future market environments, respectively.
- User comfort, power efficiency, maximum clean energy utilization, and cost minimization objectives are achieved simultaneously for both models through proposed modified multi-objective gray wolf optimization and modified multi-objective prioritized plug-and-play and knapsack algorithms.
- A cost–benefit analysis of each microgrid in the multi-microgrid paradigm is performed using parameters such as net present value, internal rate of return, return on investment, payback period, and profitability index through various tariff adjustment techniques for renewable energy resources and battery energy storage systems.

The proposed paper is organized as follows: Section 3 provides the approach adopted by researchers to model the suggested framework for each MG and implementation of the proposed study. The results of the proposed work and discussion on it are given in Section 4, and Section 5 presents the conclusion of the proposed work.

2 Methodology

2.1 Modeling of the complete MMG setup

The devices deployed as the fixed load in each MG are energy-efficient, and their financial and functional requirements determine their quantity. The simplex mode of communication (uni-directional communication) occurs between the fixed load device agent and the controller of the respective MGs. Table 1 shows the base load of smart residential microgrids (SRMGs), smart commercial microgrids (SCMGs), and smart industrial microgrids (SIMGs). Time flexible devices (TFDs) are traditionally moved away from peak times to prevent excessive prices and load constraints on their utility with maximum user comfort. These load devices are relocated to the period of extra renewable generation power in the proposed model to achieve maximum RER utilization and reduce energy curtailment. Furthermore, power flexible devices (PFDs) are optimally set in a rated range of power through an intelligent thermostat. According to the American Society of Heating, Refrigerating, and Air-Conditioning Engineers (ASHRAE) standard 55-2010, intelligent thermostats ensure that AC and HVAC systems function between 20°C and 27°C based on P_{sur}. Power flexible devices deploy duplex communication with their respective controllers. PFDs and TFDs for an MMG are given in Table 1.

In PFDs, an intelligent thermostat in HVAC and AC is fed with the P_{sur} signal and real-time temperature sensor data for 24 h by using a level 3 controller to function according to the framework based on the ASHRAE 505 standard. The use of the P_{sur} signal results in less energy

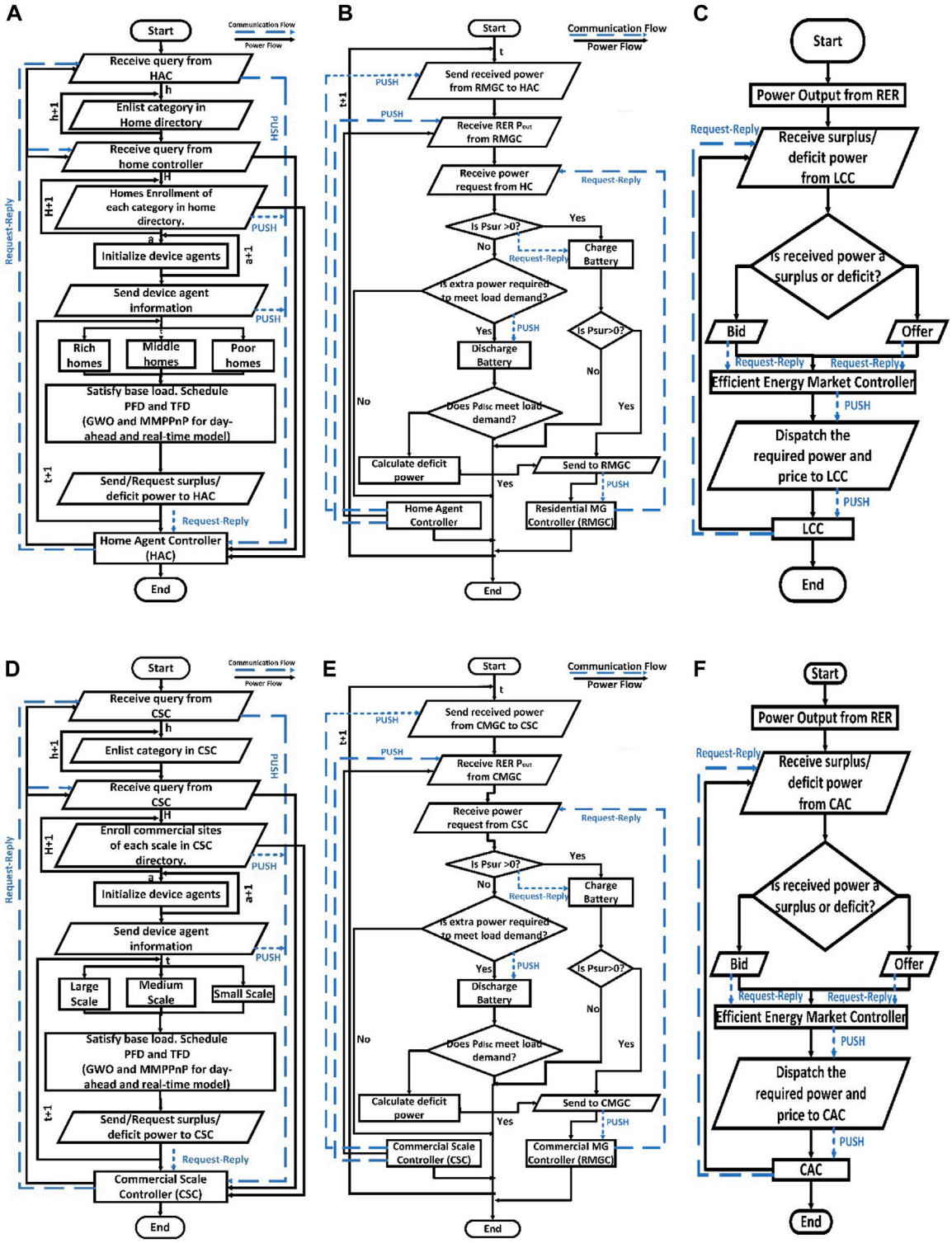

FIGURE 3
(Continued).

restriction and reliance on the traditional electric grid. The thermostat's cooling and heating functions are active 24 h a day, using real-time and day-ahead signals. The thermostat's temperature is set by an intelligent agent in response to the incoming signal. Based on the incoming P_{sur} signal from the respective controller, the thermostat agent makes an intelligent T_{pref} cooling choice. When the P_{sur} signal received is more significant than 0, the agent lowers the temperature point below T_{pref}, and the value of ΔT falls below 0. The temperature T_{pref} increases when the incoming signal P_{sur} is less than 0 and ΔT becomes more significant than 0. Similarly, an agent actively raises the thermostat's temperature

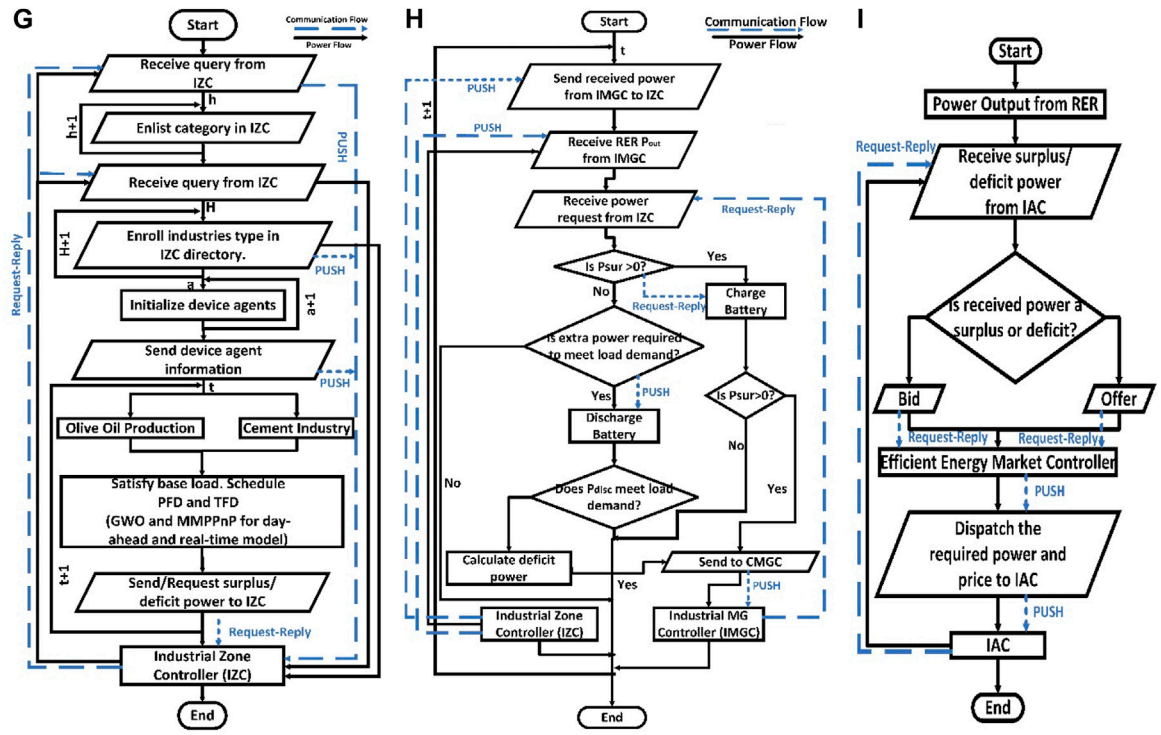

FIGURE 3
(Continued). Workflow of SRMGs: **(A)** layer 3; **(B)** layer 2; **(C)** layer 1. Workflow of SCMGs: **(D)** layer 3; **(E)** layer 2; **(F)** layer 1. Workflow of SIMGs: **(G)** layer 3; **(H)** layer 2; **(I)** layer 1.

set point P set if the incoming signal P_{sur} value is positive. In response to the negative value of P_{sur}, the temperature set point decreases to T_{upper}. T_{upper} and T_{lower} are the allowable upper and lower temperatures used for heating, defined as per the ASHRAE standard 55-2010, respectively. The mathematical representation of the thermostat is given in Eqs 1, 2:

$$T_{set,cooling,heating}(t) = T_{pref} + \Delta T, \tag{1}$$

where

$T_{set,cooling,heating}$ = *Set Room temperature at t by thermostat for cooling, heating*

T_{pref} = *preferable room temperature*

ΔT = *variation from* T_{pref},

$$\Delta T = \begin{cases} \geq T_{min,max} - T_{pref} \\ \leq T_{max,min} - T_{pref} \end{cases}. \tag{2}$$

From Figures 1A, B, the thermostat's set point oscillates between the permitted limits of temperature, T_{lower} and T_{upper}, depending upon the value of the P_{sur} signal and the mode of the thermostat. The slope of the fluctuation is given by Eqs 3–5:

$$Slope_{high} = \frac{P_{sur}}{T_{lower,upper} - T_{pref}} \quad if\ P_{sur} > 0, \tag{3}$$

$$Slope_{low} = \frac{P_{def}}{T_{upper,lower} - T_{pref}} \quad if\ P_{sur} < 0, \tag{4}$$

$$P_{sur\,(t)} = \frac{P_{sur} - \sum_{t=1}^{24} P_{sur}}{\sum_{t=1}^{24} P_{sur}}. \tag{5}$$

To ascertain the value of ΔT at any particular time t, the intelligent agent evaluates the incoming P_{sur} and observes whether it is less or more than the average value of P_{sur} over 24 h. From Eqs 6, 7, the set point temperature of the thermostat at any instant is calculated.

$$T_{set,cooling,heating}(t) = T_{pref} + \frac{P_{sur\,(t)}}{Slope_{high,low}} \quad P_{sur} > 0, \tag{6}$$

$$T_{set,cooling,heating}(t) = T_{pref} + \frac{P_{sur\,(t)}}{Slope_{low,high}} \quad P_{sur} < 0. \tag{7}$$

In the proposed paper, it has been observed from Eq. 8 that every 1°C thermostat change has a 6.4% change in the power consumption of HVAC and AC. Increasing the temperature decreases HVAC and AC load consumption for cooling purposes. Similarly, load consumption increases with the increase of 1°C. Conversely, rise and fall in temperature increase and decrease consumption for heating purposes, respectively.

$$\Delta T_{cooling} = \begin{cases} -1°C + 6.4\%\, consumption \\ +1°C \quad - 6.4\%\, consumption \end{cases};$$
$$\Delta T_{heating} = \begin{cases} +1°C + 6.4\%\, consumption \\ -1°C \quad - 6.4\%\, consumption \end{cases}. \tag{8}$$

2.2 Multi-layer MAS infrastructure for smart MMG setup

A smart residential MG is a basic model for different categories of homes based on its standard of living and load demand based on the personal comfort and poor, rich, and middle classes, as

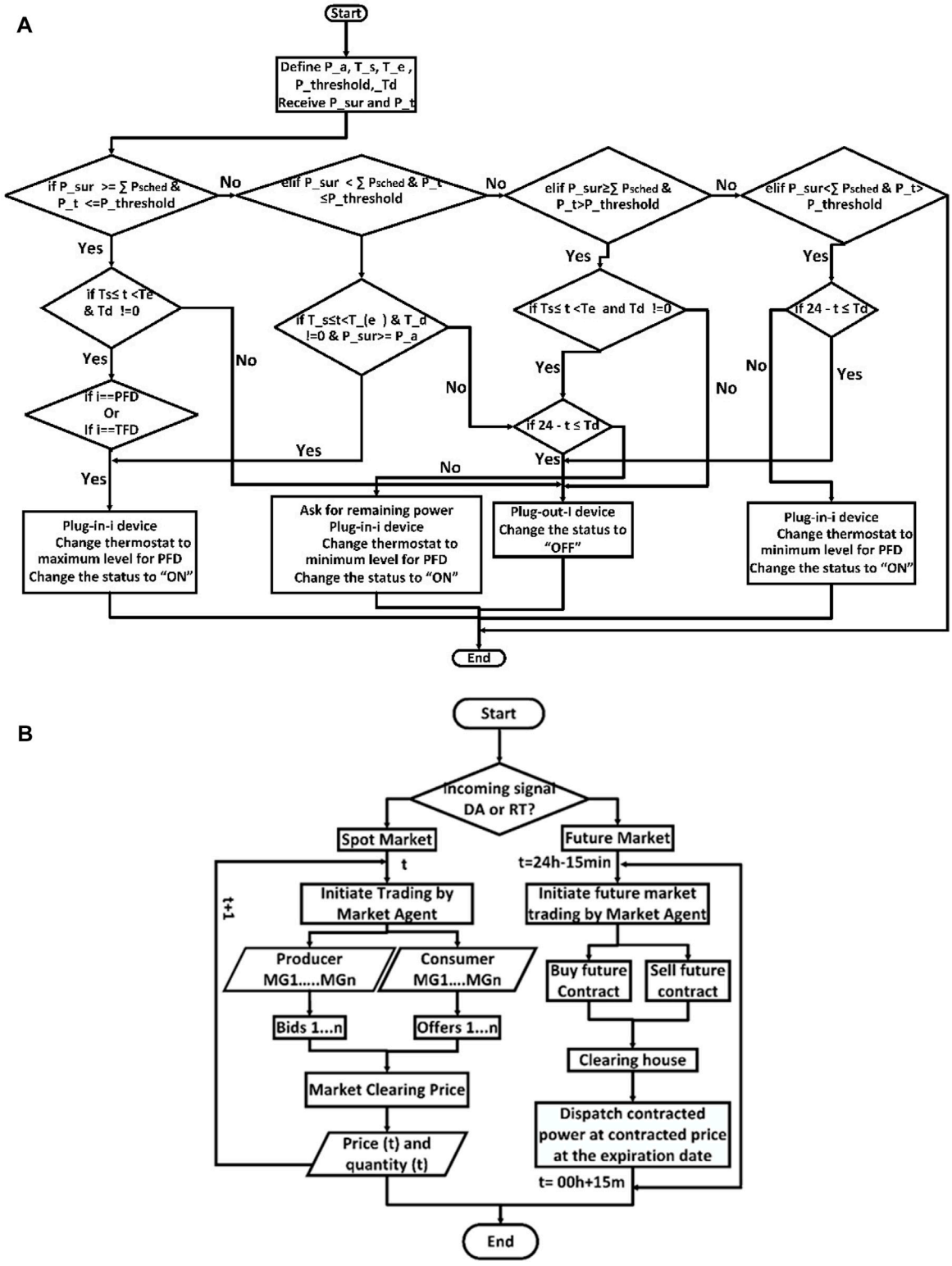

FIGURE 4
Workflow of **(A)** MMPPnP and **(B)** efficient energy management market.

demonstrated in Figure 2A. The configuration is designed for both real-time and day-ahead (DA) MG operations. The real-time approach operates based on hourly signals such as load demand, generation from RERs, and energy price. In contrast, the day-ahead model operates entirely on forecasted data for 24 h. The power needs of the occupants of the mentioned homes with respect to the

TABLE 2 Essential details related to SRMGs.

Installed RER capacities/cases	Case 1		Case 2 (base case)		Case 3	
Solar (kW)	100		200		250	
Wind (kW)	50		100		150	
Aggregated power (kW)	150		300		400	
Bid and offer/grid type			Bid ($/kWh)		Offer ($/kWh)	
Commercial			0.095		0.09	
Industrial			0.1		0.09	
Coal-fired power plant (main grid)			0.105		0.065 (FiT)	
Monthly billing/cases	Case 1		Case 2 (base case)		Case 3	
Schedule load ($)	2,425.9		2,552.2		2,667.3	
Business-as-usual (BAU) load ($)	4,487.7		4,031.9		3,844.0	
Emissions/cases	Case 1		Case 2 (base case)		Case 3	
Emissions from renewables (g/kWh)	21,671		28,539		31,390	
Emissions from the coal grid (g/kWh)	906,101		1,097,080		1,187,561	
Decrease in emissions (%)	97.60836		97.39866		97.3568	
Proposed tariff breakdown tariffs ($/kWh)	Base TOU (BT)	Half-base TOU (HBT)	Double-base TOU (DBT)	Base flat rate (BFR)	Half-base flat rate (HBFR)	Double-base flat rate (DBFR)
Renewable ON-peak generation	0.065	0.0325	0.13	0.04225	0.02112	0.0845
Renewable OFF-peak generation	0.085	0.0425	0.17	0.02975	0.01487	0.0595
Battery	0.0875	0.04375	0.175	0.075	0.04	0.145
Flat rate	0	0	0	0.072	0.036	0.144

economic diversity are increased by cost-effective alternatives subject to their affordability and various living patterns. Similarly, a smart commercial MG framework comprises different classifications depending upon the level of power consumed by each scale.

In the proposed work, three commercial-scale, namely, small, medium, and large, setups are considered for both real-time and day-ahead signals, as shown in Figure 2B. With intelligent scheduling of power and time-adaptable devices, commercial modeling addresses the priority assigned to the devices of each commercial scale, cost, and power efficiency. The schedule is done so that the work of each MG category is not disrupted. Shops, markets, buildings, agricultural land, educational institutions, and hospitals (emergency and outpatient door (OPD)) make up the commercial grid load.

In the proposed work, the smart industrial MG setup consists of high-energy-intensive cement and medium-energy-intensive olive oil industries, as shown in Figure 2C. The industrial load is intelligently scheduled through the active participation of agents in the MAS framework. It is a common observation that industries are more vulnerable to the penalties imposed on them for maximum power usage at peak times. Depending upon the feasibility, the industries are not prepared to schedule their load if the cost of not producing at a particular hour exceeds the penalties. However, in our research, industries are allowed to increase production at peak times for clean generation to fulfill the demand. Consequently, both industries achieved cost minimization, reduced production risk, and increased clean energy utilization. Furthermore, the intelligent actions of smart agents assist in achieving the industry's routine productivity and profitability matters. The MAS framework deploys advanced communication patterns and low latency rates which edify the agents to achieve their distributed objectives in a complex and secure environment. In addition, a secure transport protocol, namely, inter-process communication (IPC), is deployed for connecting agents. The modeled MAS in the proposed paper for each of the three MGs is of a hierarchical type divided into three levels.

2.2.1 Layer 3

A home agent controller (HAC) employs a request–reply communication pattern for asking about the details from the load agent devices in SRMGs. Load agent devices use the push–pull communication pattern to send the necessary information for scheduling to the HAC. Similarly, a Commercial agent controller (CAC) and an industrial zone controller (IZC) in SCMGs and SIMGs send and receive queries regarding the load details to categorized areas and zones using the

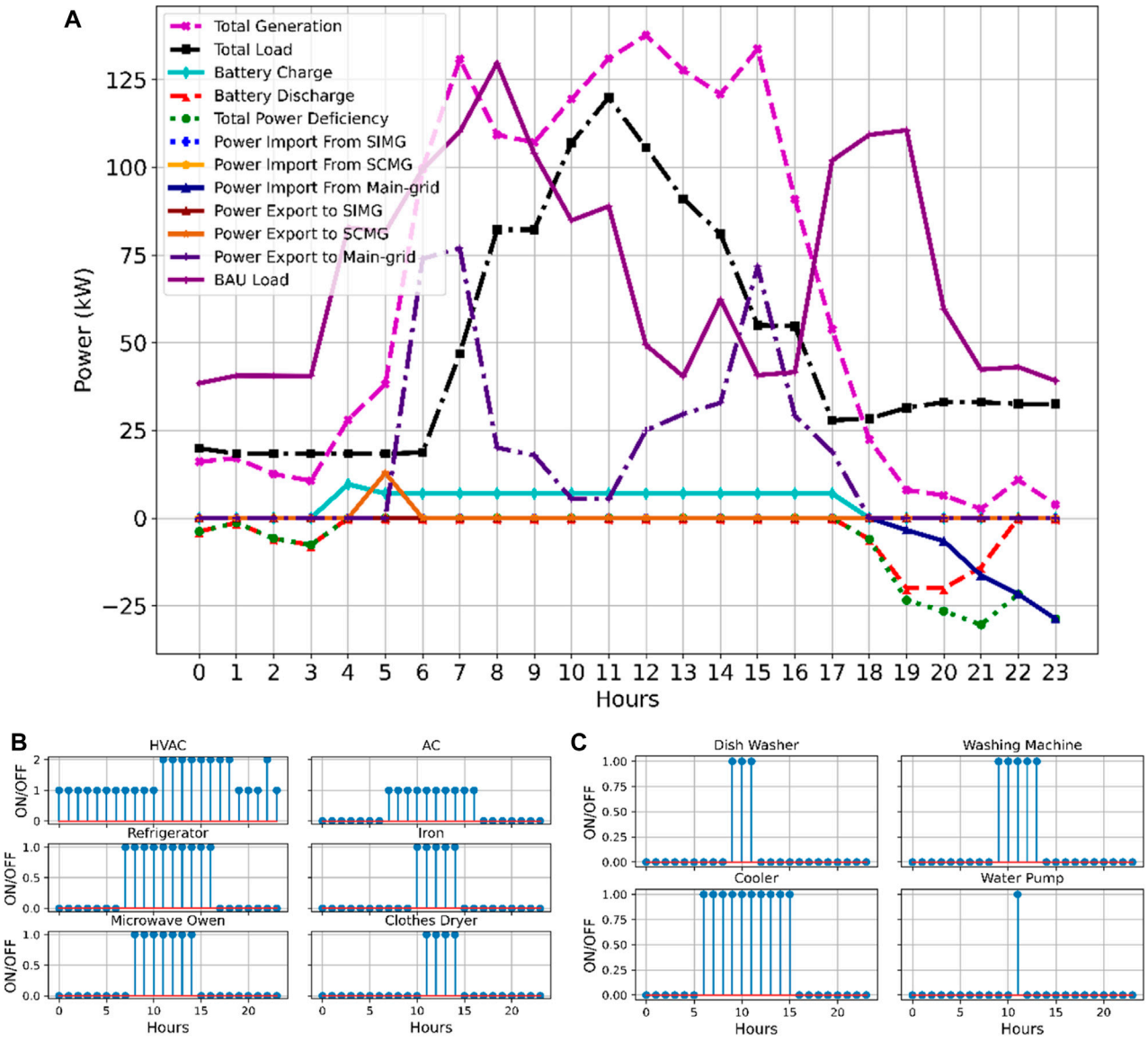

FIGURE 5
(Continued).

request–reply and push–pull communication patterns. The HAC, CAC, and IZC in SRMGs, SCMGs, and SIMGs deploy MMGWO and modified multi-objective-prioritized plug-and-play (MMPPnP) algorithms for day-ahead and real-time signals, respectively, to achieve the defined objectives, . From Eqs 9–11, $TL_{devices\ (x)}$ represents the total load of the devices attached to the HAC, CAC, and IZC in each category of the load pattern in terms of priority. The value of x determines the load category of each MG in the MMG paradigm. $L_{total\ (x)}$ provides the total load of the MG by adding the base load. $D_{priority}$ is the array of devices that represent the increasing priority of the devices. *PFD* and *TFD* represent the power of time flexible and power flexible devices. For the effective dispatching of scheduled devices to meet the DR, the total load at the ongoing time $L_{(x)_{(t)}}$ linked via agents is given by Eq. 12:

$$x = \{home\ categories = [home\ pattern\ (Rich, Middle, Poor)]\},$$

$$x = \{commercial\ categories = [Areas\,(Large, Medium, Small\ Scale)]\},$$

$$x = \{industrial\ categories = [Zones\,(High, medium\,)energy\ intensive]\},$$

$$D_{priority\ (x)} = \{P(1), P(2), \ldots .P(total.no.devices)\}, \tag{9}$$

$$TL_{devices\ (x)} = \sum_{n=1}^{no.of.PFD}\left\{\left(D_{priority}\right)(PFD_n)\right\} + \sum_{k=1}^{no.of.TFD}\left\{\left(_{D_{priority}}\right)(TFD_n)\right\} \tag{10}$$

$$L_{total\ (x)} = \sum_{t=1}^{24} B_l\,(x) + TL_{devices\ (x)}, \tag{11}$$

$$L_{(x)_{(t)}} = B_{l\ (x)\ (t)} + \left(TL_{devices\ (x)\ (t)} \times \gamma_0^1\right). \tag{12}$$

t represents the incoming signal (day-ahead or real-time). γ_0^1 gives the status (ON/OFF) of the connected devices at the

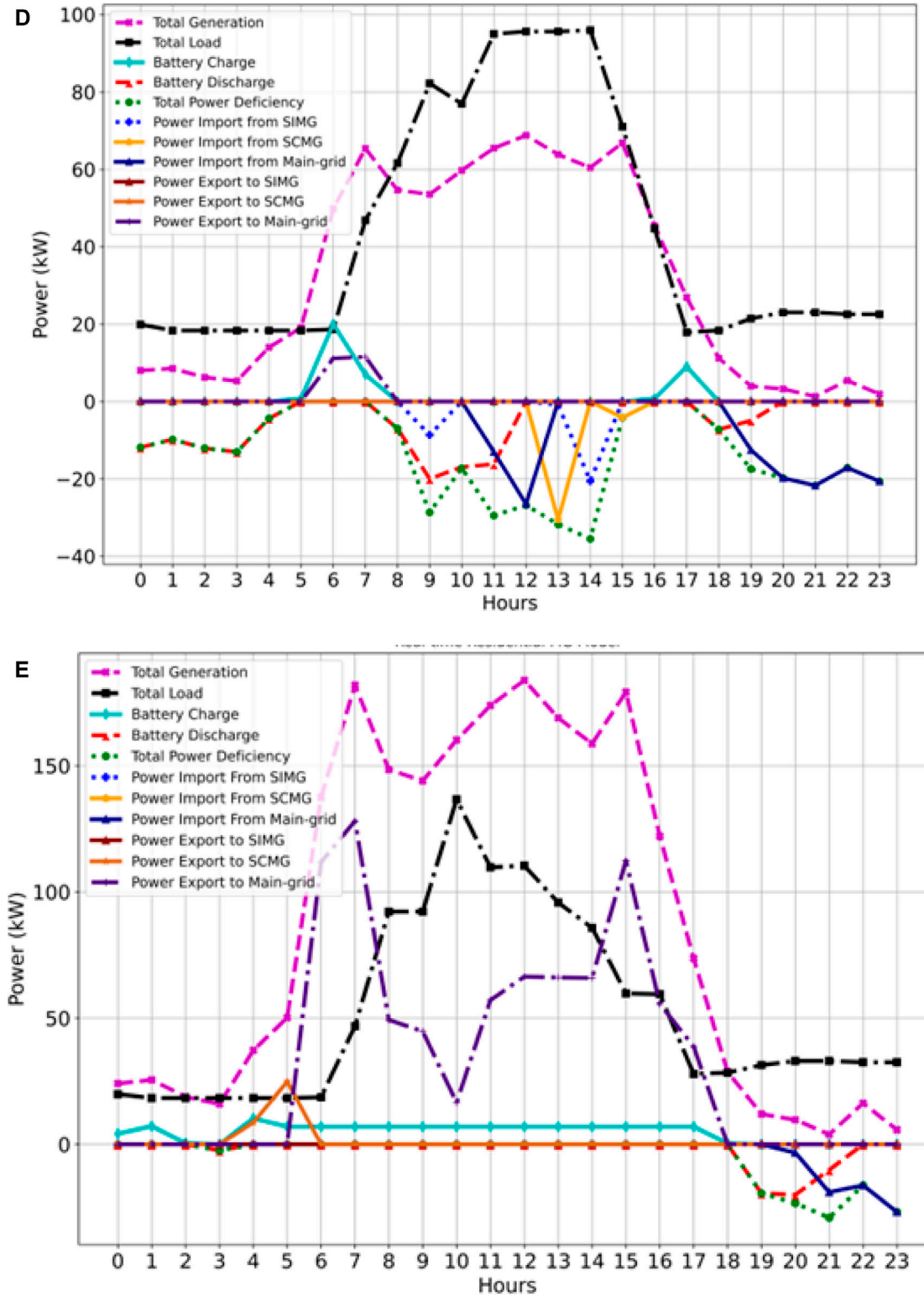

FIGURE 5
(Continued).

time frame t. As mentioned previously, $TL_{devices\,(x)\,(t)}$ gives the power of time flexible and power flexible devices at the current t for each MG in the MMG paradigm. Therefore, γ_0^1 only accounts for $TL_{devices(x)\,(t)}$. The signal of surplus generation P_{sur} triggers the ON/OFF status of a device.

10.3389/fenrg.2024.1348458

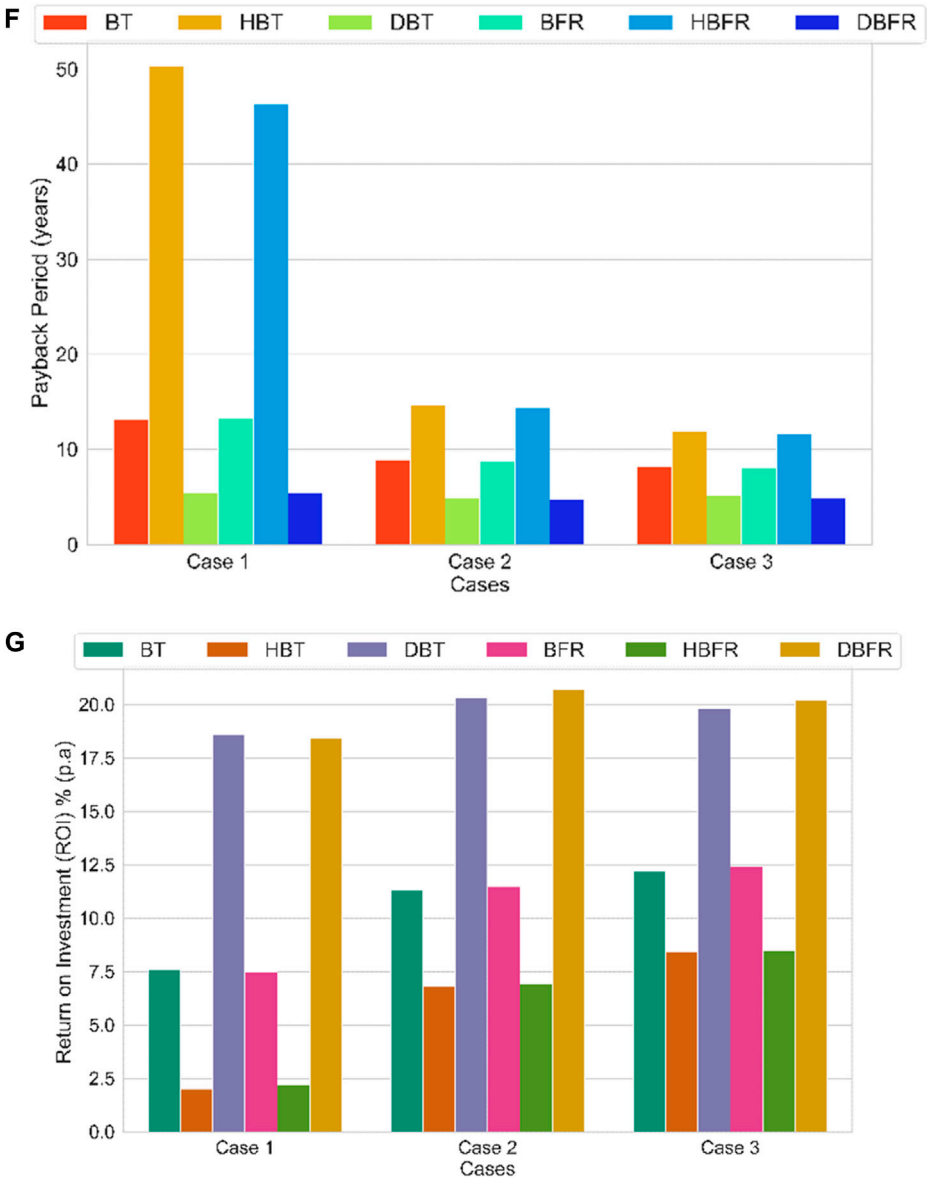

FIGURE 5
(Continued).

$$TFD_n = \begin{cases} 1, & \begin{cases} P_{sur} > 0 \\ D_{S.T} \le t \ge D_{E.T}, \\ P_t \le P_{thres} \end{cases} \\ 0, & otherwise \end{cases} \tag{13}$$

$$PFD_n = \begin{cases} 1, & \begin{cases} thermostat\ at \max level & \begin{cases} 0 < P_{sur} \ge PFD_{n_{max}} \\ D_{S.T} \le t \ge D_{E.T} \\ P_t \le P_{thres} \end{cases} \\ thermostat\ at \min level & \begin{cases} PFD_{n_{max}} > P_{sur} \ge PFD_{n_{min}}, 0 \\ D_{S.T} \le t \ge D_{E.T} \\ P_t \le P_{thres} \end{cases} \end{cases} \\ 0, & otherwise \end{cases} \tag{14}$$

Load-device agent controllers intelligently transition the mode of connected devices based on the defined restrictions in Eqs 13, 14. *TFD* is directed to turn ON when the incoming P_{sur} exceeds the consumer load. The tariff price determined at that hour should be less than the consumer's defined threshold price based on their affordability and comfort. Furthermore, each MG category determines the starting time, ending time slot, and time duration. At that instant, the instant *TFD* should be within the range of the starting and ending time and is not fully ON for the defined hours. The controller strictly monitors the parameters and makes autonomous and precise decisions for the connected devices. Similarly, the PFD thermostat intelligently adjusts the thermostat according to the incoming P_{sur} signal. Based on the above Eq. 16, the thermostat is adjusted at the maximum level when the incoming P_{sur} signal is greater than or equal to the *n* flexible device's maximum power $PFD_{n_{max}}$. Alternatively, the thermostat is set to the minimum level when the incoming P_{sur} signal is less than $PFD_{n_{max}}$ and greater than the *n* power flexible device's minimum power $PFD_{n_{min}}$. The *PFD* intelligent agent controller also considers each MG category's

10.3389/fenrg.2024.1348458

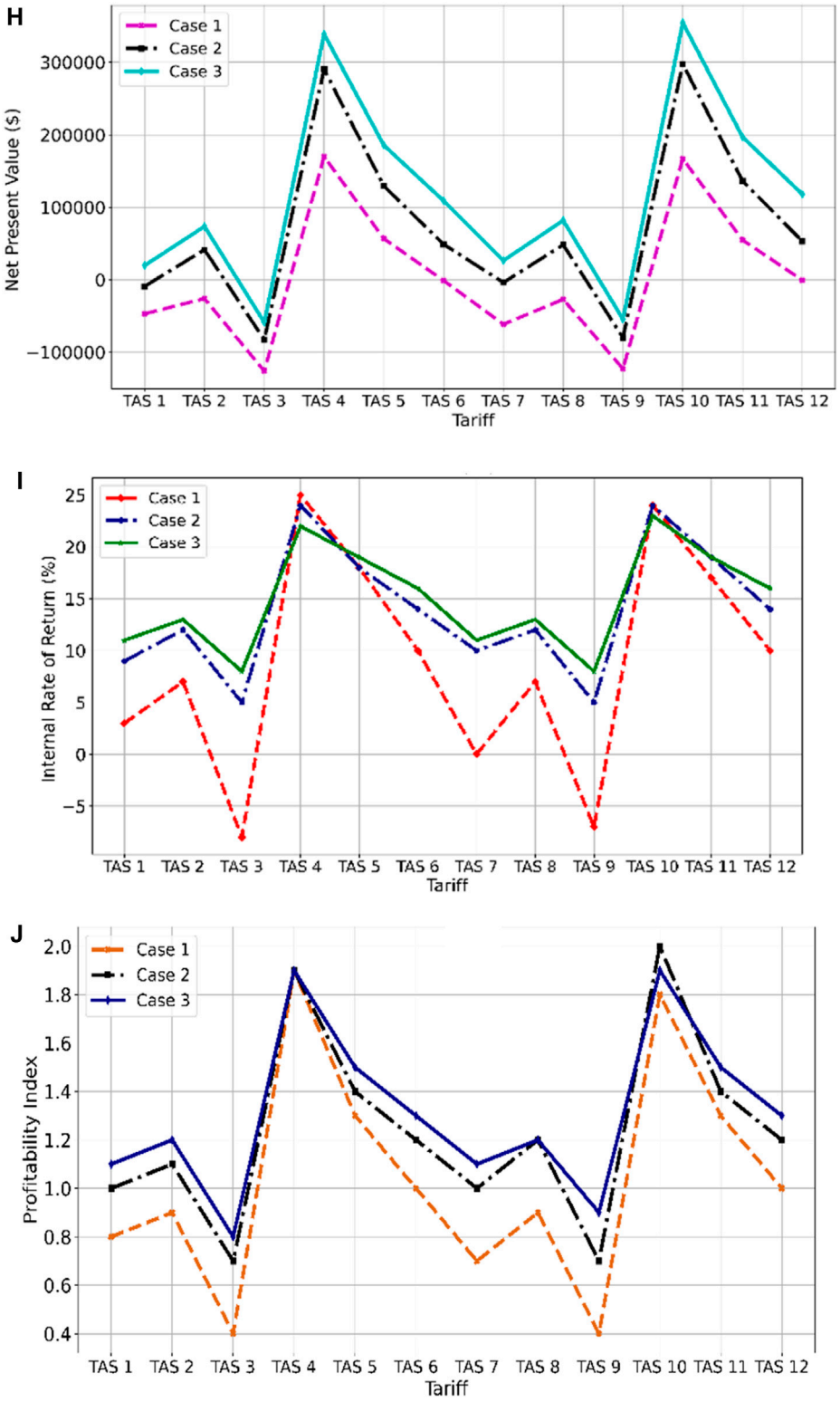

FIGURE 5
(Continued). Illustration of the RTM of SRMGs: **(A)** base case power flow; **(B)** and **(C)** base case status of schedule devices; **(D)** case 1; **(E)** case 3; CBA of the proposed tariff; **(F)** PBP; **(G)** ROI; CBA of the proposed tariff adjustment strategy (TAS); **(H)** NPV; **(I)** IRR; **(J)** PI.

cost and time limits when scheduling devices. The workflow of layer 3 in SRMGs, SCMGs, and SIMGs is demonstrated in Figures 3A, D, G, respectively.

2.2.2 Layer 2

This layer comprises a local community controller (LCC) in SRMGs, CAC in SCMGs, and IAC in SIMGs. Each MG constitutes

TABLE 3 Proposed tariff adjustment strategy (TAS) for the MMG.

Tariff adjustment strategy	TAS 1	TAS 2	TAS 3	TAS 4	TAS 5	TAS 6	TAS 7	TAS 8	TAS 9	TAS 10	TAS 11	TAS 12
Tariff structure for 25 years	Base TOU tariff PB. Half-base TOU tariff onward	Base TOU tariff for 25 years	Half-base TOU tariff for 25 years	Double-base TOU tariff for 25 years	Double-base TOU tariff PB. Base TOU tariff onward	Double-base TOU tariff PB. Half-base flat rate tariff onward	Base-flat rate tariff PB. Half-base flat rate tariff onward	Base flat rate tariff for 25 years	Half-base flat rate tariff for 25 years	Double-base flat rate tariff for 25 years	Double-base flat rate tariff PB. Base flat rate tariff onward	Double-base flat rate tariff PB. Half-base flat rate tariff onward

TABLE 4 Essential details related to SCMGs.

Installed RER capacities	Case 1	Case 2 (base case)	Case 3
Solar (kW)	400	500	550
Wind (kW)	400	500	550
Aggregated power (kW)	800	1,000	1,100
Bid and offer/grid type		Bid ($/kWh)	Offer ($/kWh)
Residential		0.09	0.095
Industrial		0.1	0.095
Coal-fired power plant (main grid)		0.105	0.07 (FiT)
Monthly billing/cases	Case 1	Case 2 (base case)	Case 3
Schedule load ($)	14,410.5	13,075.1	7637.8
BAU load ($)	14,978.7	13,875.8	13,838.2
Emissions/cases	Case 1	Case 2 (base case)	Case 3
Emissions from RER (g/kWh)	111,881	116,104	118,071
Emissions from the coal grid (g/kWh)	4,732,576	4,771,981	4,779,022
Decrease in emissions (%)	97.635931	97.56697	97.52939

Proposed tariff breakdown tariffs ($/kWh)	Base TOU (BT)	Half-base TOU (HBT)	Double-base TOU (DBT)	Base flat rate (BFR)	Half-base flat rate (HBFR)	Double-base flat rate (DBFR)
REG ON-peak	0.07	0.035	0.14	0.0455	0.02275	0.091
REG OFF-peak	0.09	0.045	0.18	0.0315	0.01575	0.063
Battery	0.0925	0.04625	0.185	0.08	0.04	0.155
Flat rate	0	0	0	0.077	0.0385	0.154

the BESS with different capacities in the proposed paper. Because of the intricate numerical computations and intelligent decisions executed by the agents in this layer, it has core importance. Layer 2 serves as a link between the consumer and generational levels. Consequently, this layer acts both as a sink and a source across the 24-h operation of agents. Layer 2 controllers for each MG use a request–reply pattern for communication with the BESS, layer 1, and layer 3. At each time period (per hour), the layer 2 controllers obtain power consumption and power generation signals simultaneously from the respective MGs. Controllers calculate the demand/generation power difference from the received power signals and decide the power status using a knapsack algorithm. Priorities are assigned to receiving power utilization by the LCC, CAC, and IAC, as shown in Eq. 15, in the proposed research. The operation of devices is explained based on a four-tiered priority list assigned by the PPnP. Figures 3B, E, H show the workflow of layer 2 in SRMGs, SCMGs, and SIMGs, respectively. The mathematical representation of power at layer 2 is represented in Eqs 16, 17:

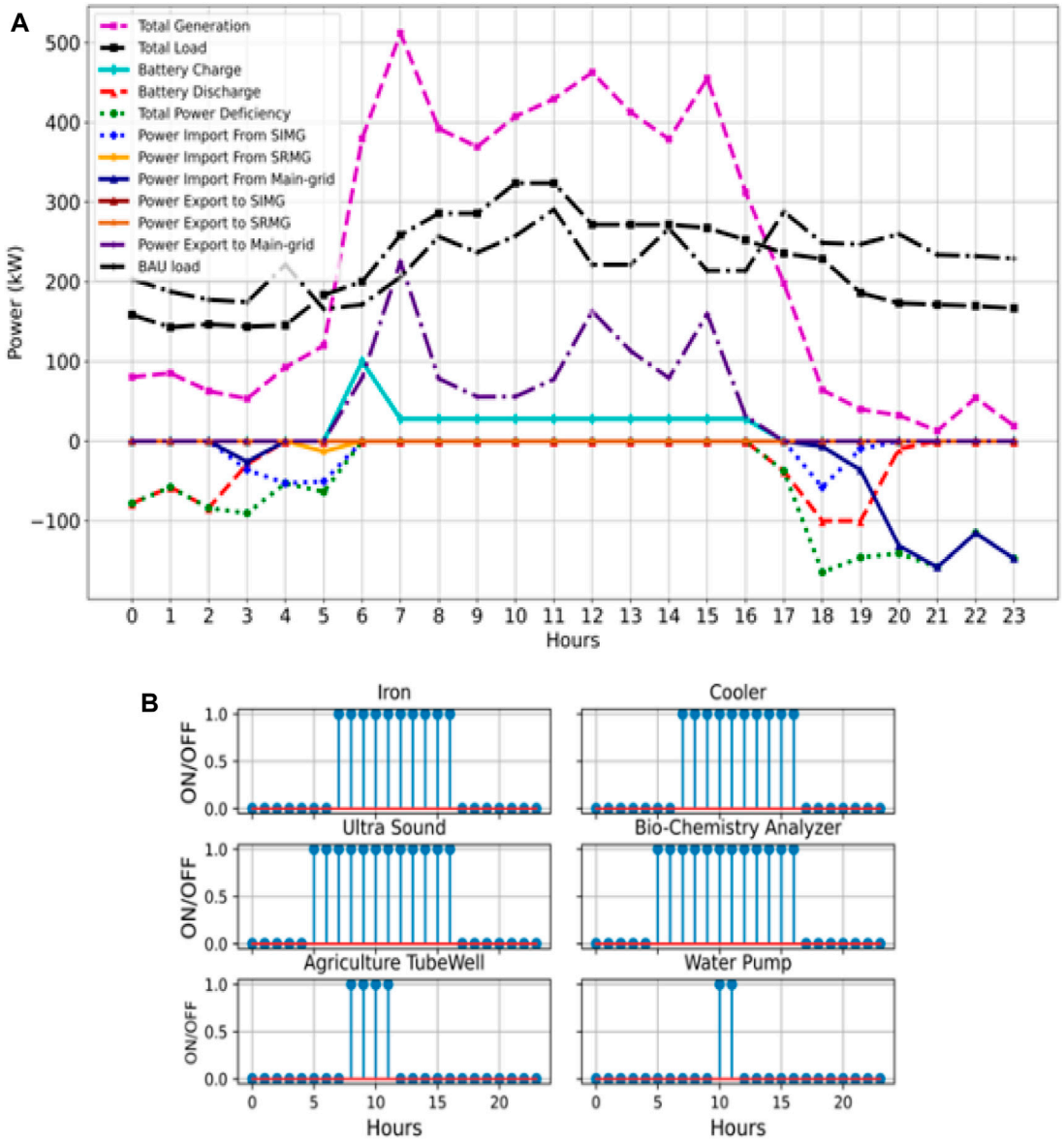

FIGURE 6
(Continued).

$$\begin{bmatrix} P_{priority}(1) = & Fixed/BaseLoad \\ P_{priority}(2) = & Scheduled\ Load_{TFD/PFD} \\ P_{priority}(3) = & BESS \\ P_{priority}(4) = & Market\ Controller \end{bmatrix}, \tag{15}$$

$$P_y = \left(P_{source_{(t)}} - \left(B_{l(x)(t)} + TL_{devices(x)_{(t)}}\right)\right), \tag{16}$$

$$P_{BESS} = P_y \begin{cases} +ive\,(\gamma^1) \\ -ive\,(\gamma^0) \end{cases}. \tag{17}$$

y represents the power received by the LCC, CAC, and IAC deployed in layer 2 for SRMGs, SCMGs, and SIMGs, respectively. The aggregated power consumption of each MG with the battery acting as a sink at any instance t is given by the following Eq. 18:

$$P_{y(total)} = P_y + P_{BESS}. \tag{18}$$

2.2.3 Layer 1

Layer 1, as shown in Figures 3C, F, I, acts as a gateway among RERs, MGs through the energy market, and level 2 systems. Layer 1 constitutes the Residential micro-grid controller (RMGC) in SRMGs, Commercial micro-grid controller (CMGC) in SCMGs, and Industrial micro-grid controller (IMGC) in SIMGs. Additionally, solar agents (SAs) and wind agents (WAs) are also deployed in layer 1. RMGC, CMGC, and IMGC are the primary controllers in layer 1 and are involved in maximizing the efficiency and utilization of RERs of the respective MGs. Furthermore, it actively participates in energy trading with the primary grid and other nearby microgrids on the surplus and deficit power. In the case of P_{def}, RMGC, CMGC, and IMGC define a priority list, as that given in the following equations, which is based on cost and emission minimization. The knapsack takes optimal decisions

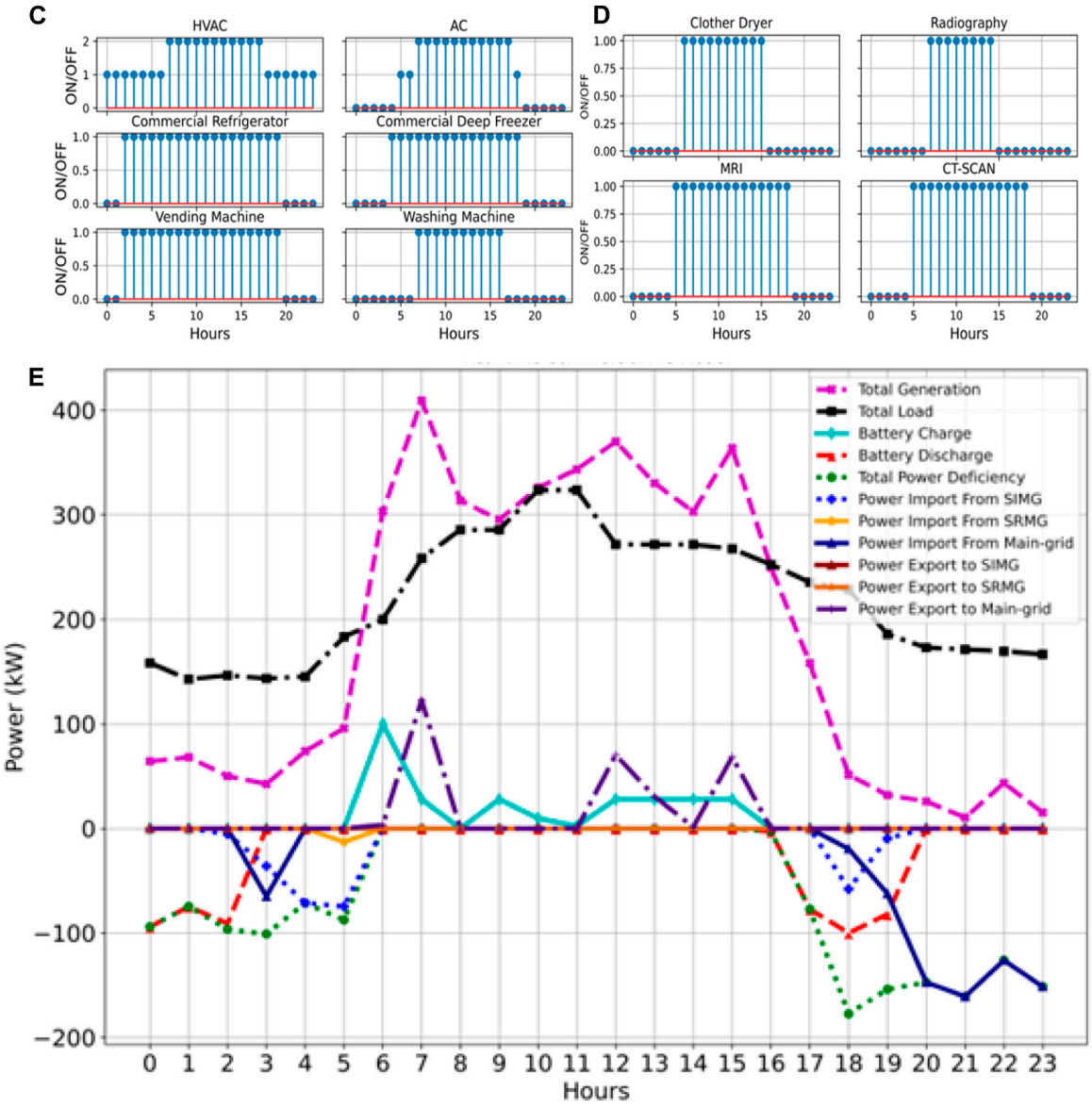

FIGURE 6
(Continued).

regarding power import deployed in layer 1 of each MG, as shown in Eqs 19–22, based on the necessity priority mentioned in Eq. 23:

$$knapsack = (weight, value, number), \tag{19}$$

$$P_{z\ (total\ gen)}(t) = \left(\sum_{1}^{m} P_y(t)\right) + P_{MG(i),main\ grid}(t), \tag{20}$$

$$P_{import} = P_y \times N_i(t) \times \gamma_0^1, \tag{21}$$

$$\begin{pmatrix} Priority\ (1) = MG(i) \\ Priority\ (2) = main\ grid \end{pmatrix}, \tag{22}$$

$$Ni_{SRMG} = \begin{cases} 1 \rightarrow Power\ outage \\ 0.9 \rightarrow Base\ load \\ 0.7 \rightarrow Residential\ emergency\ needs \\ 0.2 \rightarrow Home\ Luxury\ needs \end{cases};$$

$$Ni_{SCMG} = \begin{cases} 1 \rightarrow Hospital\ needs \\ 0.9 \rightarrow Defence\ organization \\ 0.8 \rightarrow Educational\ institution \\ 0.7 \rightarrow offices \\ 0.5 \rightarrow commercial\ buildings \\ 0.2 \rightarrow markets, shops \end{cases} \tag{23}$$

$$Ni_{SIMG} = \begin{cases} 1 \rightarrow Emergency\ Situation \\ 0.5 \rightarrow Appliances\ operation \end{cases}.$$

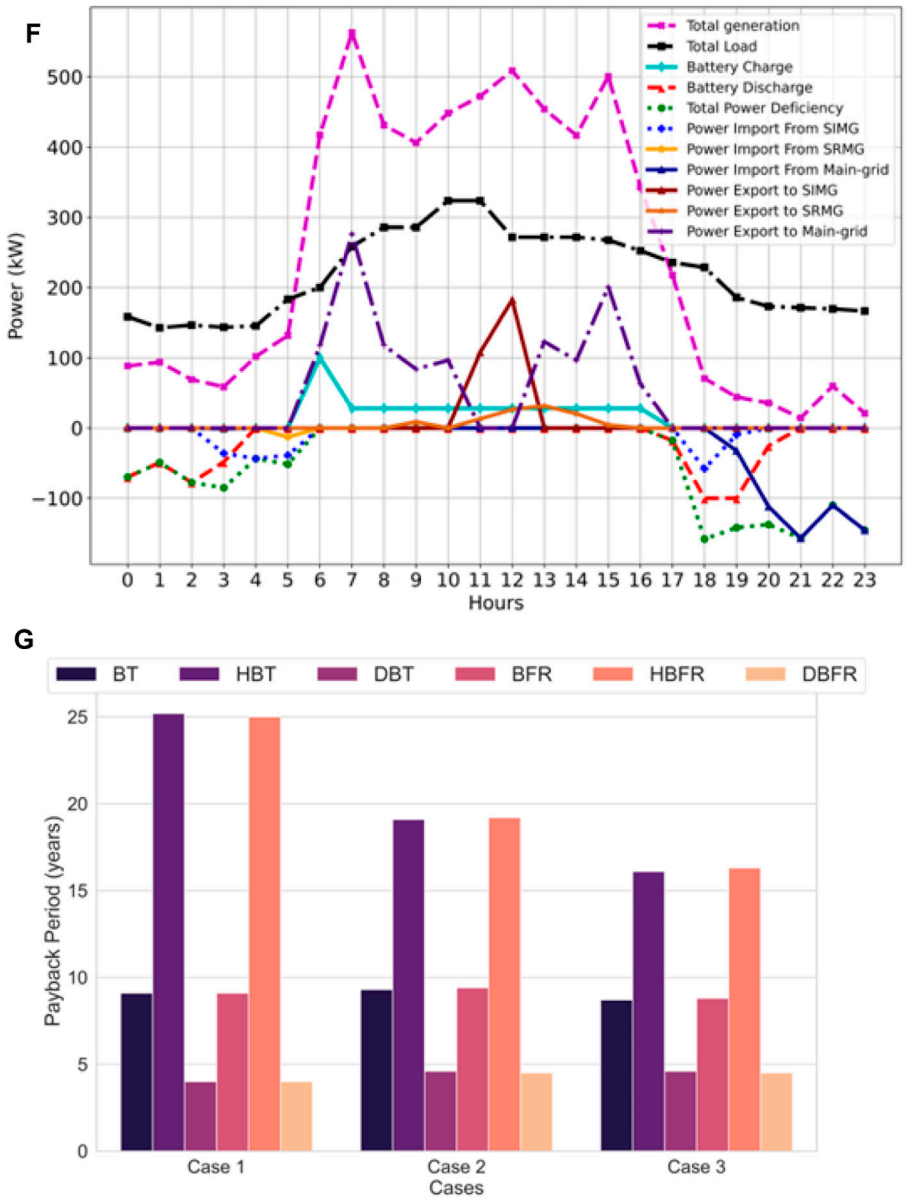

FIGURE 6
(Continued).

z represents the RMGC, CMGC, and IMGC, and $P_{z\,(total\,gen)}$ shows the RER power received by each MG. The RMGC, CMGC, and IMGC employ a request–reply pattern for communicating with RERs and layer 2 in SRMGs, SCMGs, and SIMGs, respectively. A synced publish–subscribe channel is used for taking part in REMMC activities. The solar and wind power output at any instant t is calculated using Eqs 24, 25 (Malik et al., 2020):

$$PV_{solar}(t) = \left(\frac{G(t)}{1000}\right) \times P_{rated,1000} + \eta MPPT, \tag{24}$$

where

$G(t) = hourly\ incoming\ solar\ irradiance\ at\ 90°\ angle\ \ (W/m^2)$

$\eta MPPT = conversion\ efficiency\ of\ the\ PV\ system's\ converter$

$P_{rated,1000} = Per\ PV\ \ array\ rated\ power\ at\ 1000\ w/m^2$

From Eq. 25, the speed of wind at real-time t is given by v, whereas P_{max} is the maximum power that can be extracted from the wind turbine, and P_{furl} is the extracted output power at the cutout speed.

$$P_{wind} = \begin{cases} 0 & v_{cutout} < v < v_{cutin} \\ P_{max}\left(\dfrac{v - v_{cutin}}{v_{rated} - v_{cutin}}\right)^3 & v_{cutin} < v < v_{rated} \\ P_{max} + \left(\dfrac{P_{furl} + P_{max}}{v_{cutin} - v_{rated}}\right) & v_{rated} < v < v_{cutin} \end{cases}. \tag{25}$$

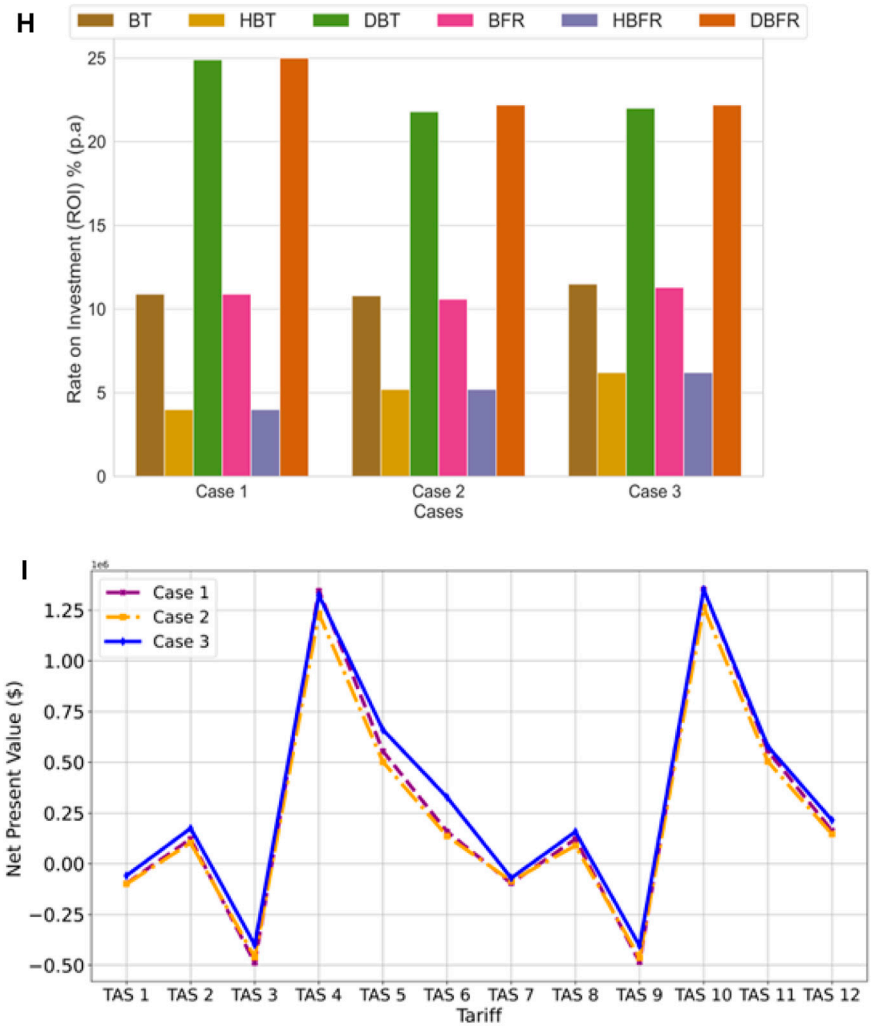

FIGURE 6
(Continued).

2.3 BESS

To encounter the volatile nature and ensure maximum utilization of the output power of RERs, we accommodate the BESS to supply supplementary services. The BESS stores surplus energy at the time of maximum or surplus generation and uses it afterward to satisfy the required demand during minimal generation or emergencies. Additionally, the cost of power is minimized by ignoring the power import from another microgrid or the primary grid. The BESS communicates with the layer 2 controller of each MG through a secure and fast channel using the push–pull communication pattern. As given in Eq. 15, the proposed paper has given the BESS the third priority for employing the RER output power. The battery deployed in the proposed paper is a lithium-ion battery (LIB). Lithium-ion batteries are most popular because of their high energy density, extended lifespan, and high cost and performance efficiency (Hannan et al., 2017). The agent associated with the BESS effectively monitors the performance measuring the parameters such as state-of-charge (SOC), depth-of-discharge (DoD), and round-trip-efficiency (RTE) and ensures the safe and reliable operation of the battery. For per hour along with 24 h, the state-of-charge of the battery is determined from the net power P_{batt} present in the battery, round-trip-efficiency η_{RTE}, and maximum capacity $E_{max.cap}$, also known as the rated capacity, and is mathematically represented in Eq. 26. The PPnP algorithm is deployed by the BESS agent to smartly observe the charging and discharging of a battery given in Eqs 27–33. The BESS agent examines the incoming surplus power and takes appropriate action based on the situation.

$$SoC\,\%\,(t) = \left(\frac{\int_{t=1}^{t=24} P_{batt}(t)\eta_{RTE}\,dt}{E_{max.cap}} \right) \times 100. \tag{26}$$

Only the power capacity P_{cap} can be used to charge the battery $P_{ch}(t)$ from the available power $P_{avail}(t)$. Similarly, the battery can discharge $P_{disc}(t)$ only P_{cap} for the necessary power $P_{use}(t)$.

$$P_{avail}(t) = P_{sur}(t) \times \eta_{ch} \times \delta_0^1 \; if \quad \{SoC < E_{max.cap}, \tag{27}$$

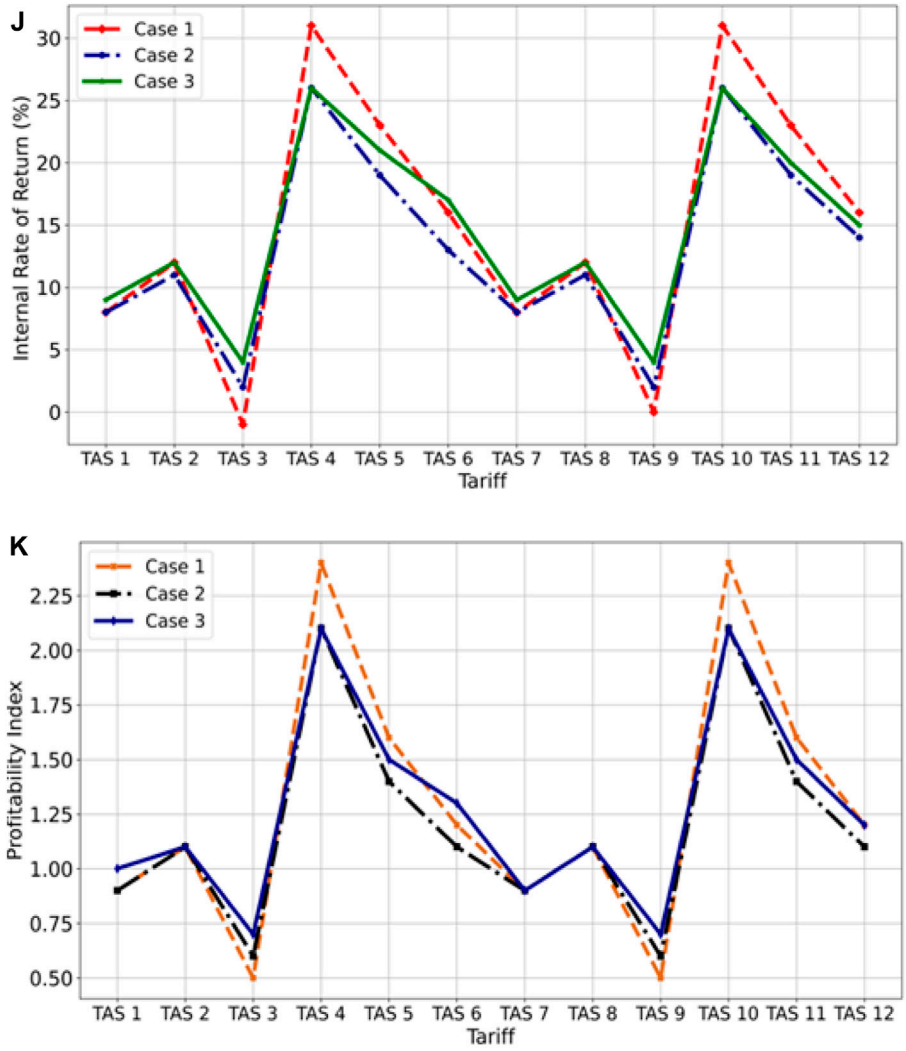

FIGURE 6
(Continued). Illustration of the RTM of SCMGs: **(A)** base case power flow; **(B)**, **(C)**, and **(D)** base case status of schedule devices; **(E)** case 1; **(F)** case 3; CBA of the proposed tariff; **(G)** PBP; **(H)** ROI; CBA of the proposed TAS; **(I)** NPV; **(J)** IRR; **(K)** PI.

$$P_{ch}(t) = P_{avail}\left(\left(P_{cap}\right)\right) if \left\{P_{avail}(t) \geq P_{cap}, \quad (28)$$

$$P_{ch}(t) = P_{avil}(t)\ if \left\{P_{avail}(t) < P_{cap}, \quad (29)$$

$$P_{use}(t) = P_{def}(t) \times \eta_{disc} \times \delta_0^1\ if \left\{E_{min.cap} < SoC \leq E_{max.cap}, \quad (30)$$

$$P_{disc}(t) = P_{use}\left(\left(P_{cap}\right)\right) if \left\{P_{use}(t) \geq P_{cap}, \quad (31)$$

$$P_{disc}(t) = P_{use}(t)\ if \left\{P_{use}(t) < P_{cap}, \quad (32)$$

$$E_{min.cap} \leq SoC\,\%\,(t) \leq E_{max.cap}. \quad (33)$$

2.4 Framework and algorithms

The proposed algorithm intends to achieve goals such as prioritizing and optimizing green energy utilization, increasing user comfort, and lowering consumer bills and greenhouse gas emissions. This suggested framework is unique, in that it achieves all of the objectives at the same time, delivering a futuristic and practical approach to the multi-microgrid paradigm.

2.4.1 Environment for modeling and developing the MAS framework

A Python-based unique and adaptive environment is developed for operating the MAS in the current work. osBrain is an OpenSistemas-designed Python-based library employed for creating and communicating agents in an MAS. osBrain facilitates the configuration of agents to adopt durable, innovative, and dynamic complex multi-hierarchical formations. The agents deployed using this library operate in real-time, autonomously, with vital intelligence, effective control, and safe communication capabilities. For agents to communicate information in an MAS, the brain provides basic communication patterns such as push–pull, request–reply, and publish–subscribe, as well as sophisticated communication patterns such as the asynchronous request–reply channel and the synced publish–subscribe channel.

TABLE 5 Essential details related to SIMGs.

Capacities of the installed RER/cases	Case 1	Case 2	Case 3 (base case)
Solar (kW)	600	400	1,000
Wind (kW)	600	400	1,000
Aggregated power (kW)	1,200	800	2,000
Bid and offer		Bid ($/kWh)	Offer ($/kWh)
Commercial		0.095	0.1
Residential		0.09	0.1
Coal-fired power plant (main grid)		0.105	0.075 (FiT)
Monthly billing/cases	Case 1	Case 2	Case 3 (base case)
Schedule load ($)	7,233.21	7,168.4	7,347.1
BAU load ($)	8,114.1	8,412.7	7,613.2
Emissions/cases	Case 1	Case 2	Case 3 (base case)
Emissions from RERs (g/kWh)	72,614	67,899	88,294
Emissions from the coal grid (g/kWh)	2,595,963	2,591,943	3,156,523
Decrease in emissions (%)	97.2028	97.3804	97.2028

Proposed tariff breakdown tariffs ($/kWh)	Base TOU (BT)	Half-base TOU (HBT)	Double-base TOU (DBT)	Base flat rate (BFR)	Half-base flat rate (HBFR)	Double-base flat rate (DBFR)
REG ON-peak	0.075	0.0375	0.15	0.04875	0.024375	0.0975
REG OFF-peak	0.095	0.0475	0.19	0.03325	0.016625	0.0665
Battery	0.0975	0.04875	0.195	0.085	0.045	0.165
Flat rate	0	0	0	0.082	0.041	0.164

The developed MAS framework deploys scenario-based communication, as mentioned above. Inter-process communication is a transport protocol for communication and data or power interactions among agents. Furthermore, osBrain uses many Python packages such as NumPy, SciPy, time, and Matplotlib for visual analysis and numerical data computation. To avoid unwanted organizations from compromising the MAS, osBrain provides secure and trusted networks for the agents to share information. The proposed MAS in the MMG paradigm is developed with the assistance of the osBrain module by employing multiple communication methods and networks depending on circumstances. The concept of object-oriented programming (OOP) in Python is also deployed for accessing programmed functions of agents in real-time scenarios.

2.4.2 Gray wolf optimization

Gray wolf optimization (GWO), introduced in Mirjalili et al. (2016), is one of the most effective meta-heuristic optimization algorithms. Because of the extreme precision of the solution, the reduced computing strain, and the minimization of slow convergence, GWO leads to other meta-heuristic algorithms such as the genetic algorithm (GA), African buffalo optimization (ABO), particle swarm optimization (PSO), binary particle swarm optimization (BPSO), and central force optimization (CFO) (Haseeb et al., 2020). This meta-heuristic algorithm mimics gray wolves' natural command structure and hunting procedure. The alpha wolf position is regarded as the fittest and best solution in the proposed MMGWO with the following objective functions:

$$objectives = maximize(UC, utilization\ of\ RER, Power\ Efficiency) = minimze(emissions, cost, power\ import\ from\ grid).$$

2.4.3 Modified multi-objective prioritized plug-and-play

Modified multi-objective-prioritized plug-and-play is an iterative method that, at each iteration, produces the best result under the defined limitations, which is then fed to the controllers for deployment. The objective of this approach is to effectively utilize the RER generation, reduce consumer bills, maximize the user's comfort, and increase the power efficiency of the devices. For achieving these objectives, certain conditions are imposed on the controller. Consequently, an intelligent controller makes autonomous decisions while considering the constraints that lead to plug-in/plug-out devices. The proposed research implements MMPPnP in a real-time model for 24 h with per-hour signals. Figure 4A explains the working flow of MMPPnP. The objectives of the proposed work are given below.

$$objectives = maximize(UC, utilization\ of\ RER, Power\ Efficiency) = minimze(emissions, cost, power\ import\ from\ grid).$$

2.4.4 Knapsack

To reduce costs and emissions while increasing UC and RER utilization, generation and storage in the algorithm are carried out according to the demand dispatch and DR pattern scheduling at the chosen periods using the multiple knapsack problem (MKP) criteria

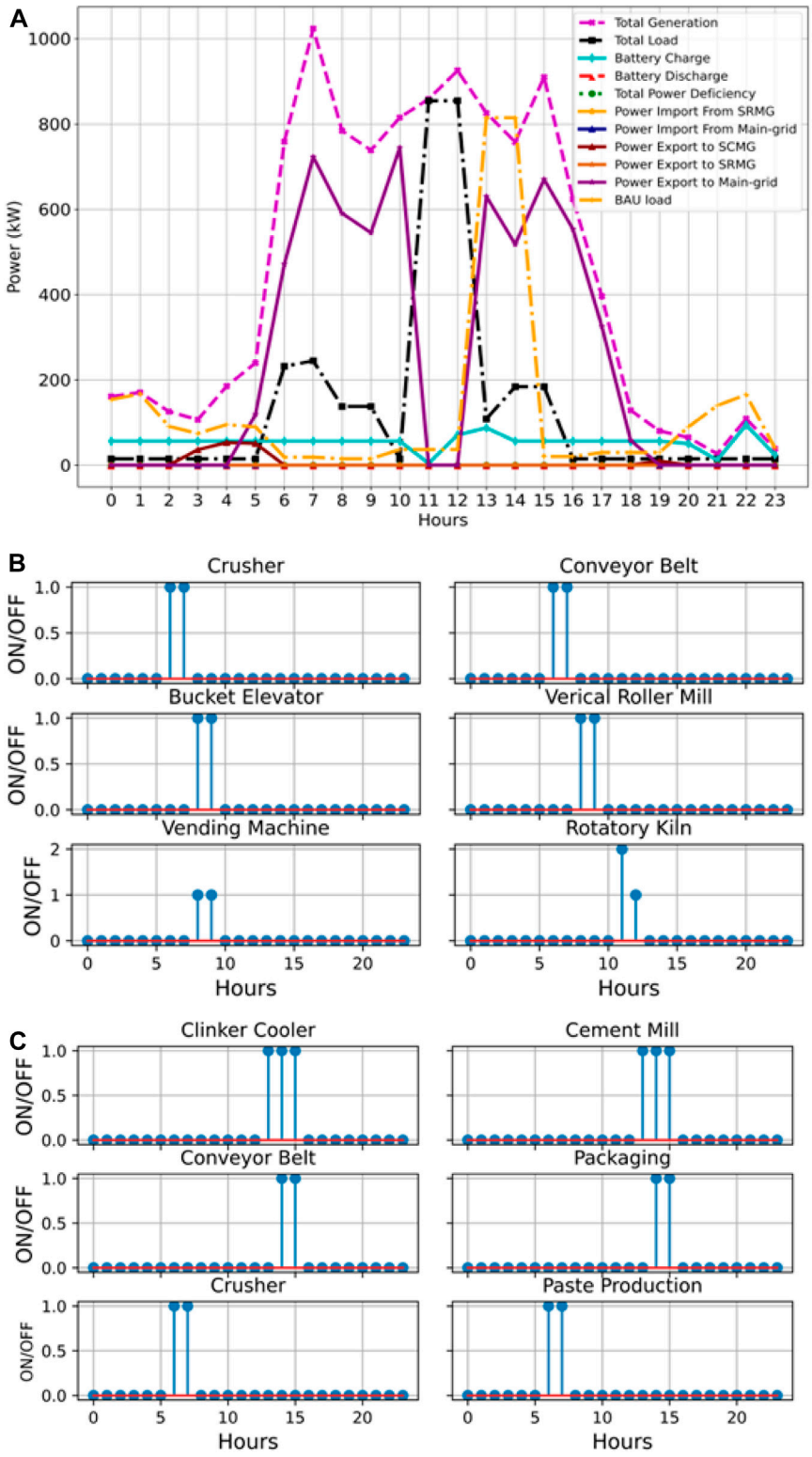

FIGURE 7
(Continued).

(Zhong et al., 2022). MKP deployment for resource allocation with "m" resources (capacities), a set of "n" objects, and "j" number of knapsack maps projected the problem accordingly (Karimi et al., 2023). The proposed work develops a constraint to limit the power usage based on the load profile and its states given in Eqs 34, 35:

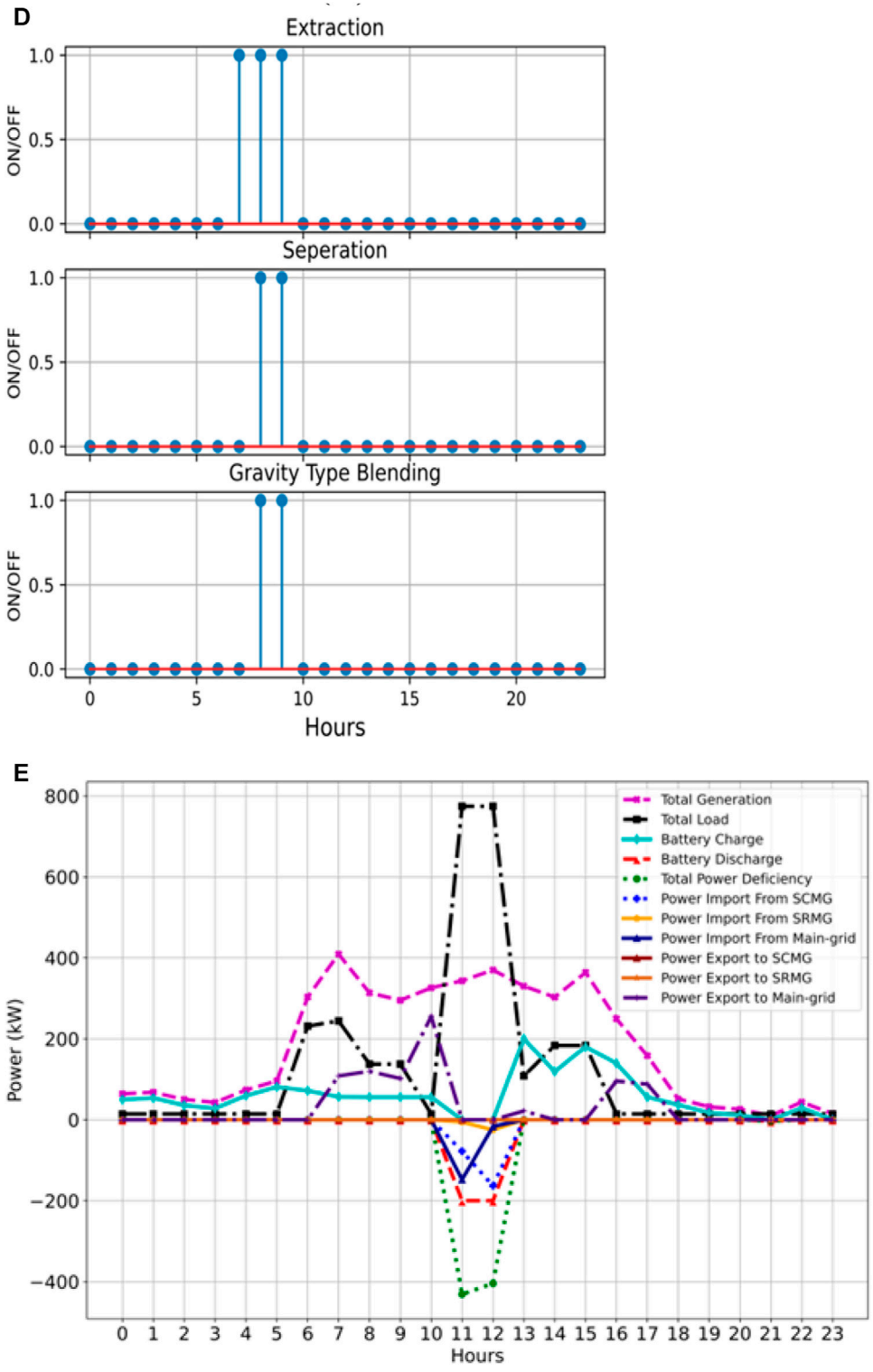

FIGURE 7
(Continued).

$$\mathrm{Cons}(t) \times \chi(t) \le C(t), \tag{34}$$

where $\chi(t) = binary\ state\ [0,1]\ of\ appliances\ at\ each\ hour, C(t) = per\ hour\ power\ capacity, Cons(t) = permitted\ consumption\ to\ selected\ appliances,$

$$\mathrm{Gen}(t) \times \chi(t) \le g(t), \tag{35}$$

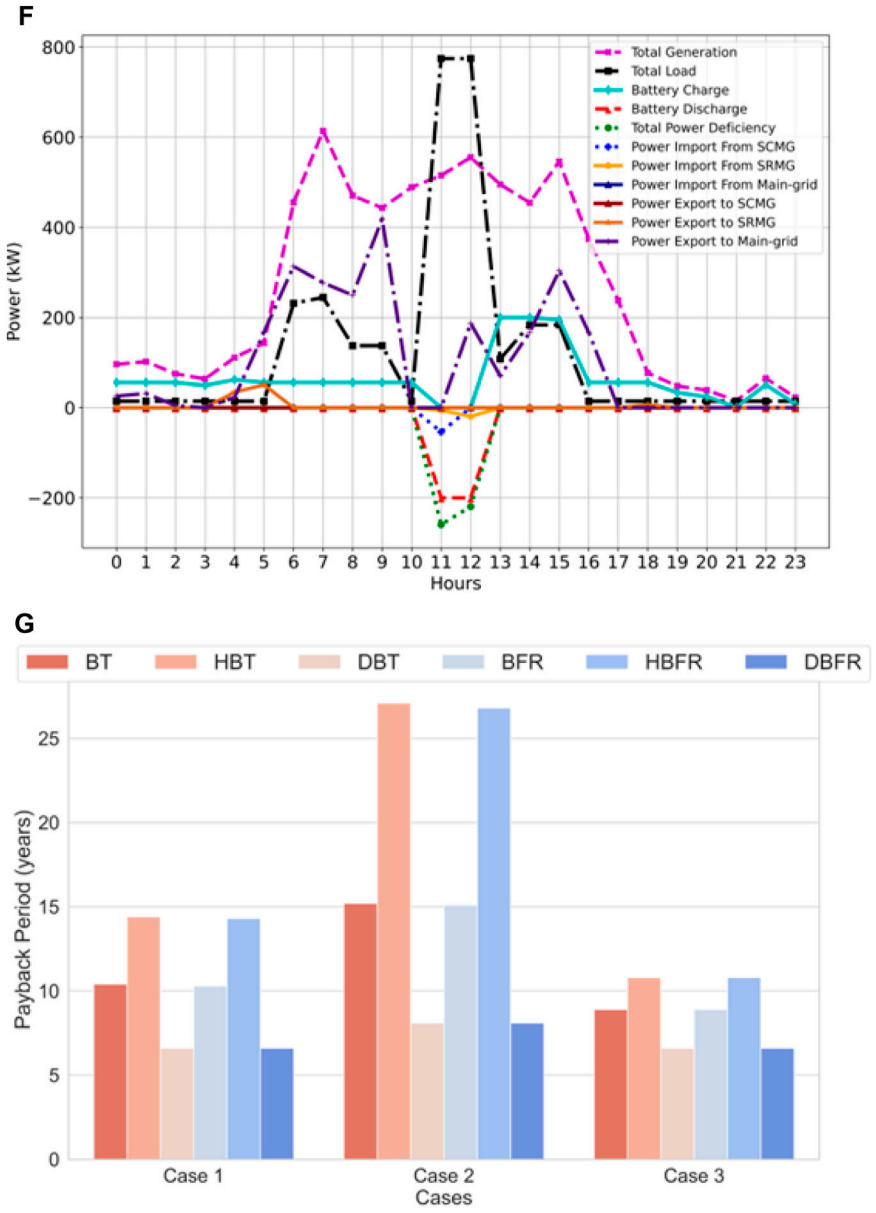

FIGURE 7
(Continued).

where
$\chi(t)$ = *binary state* $[0,1]$ *of generation soruces at each hour*
$g(t)$ = *hourly power generation available from integrated power generation soruces*
Gen (t) = generation dispatched by each generating plant

2.4.5 Efficient energy management market

The conventional infrastructure only enables a one-direction power flow from the generator to the end user, without any response. On the other hand, modern advanced grids provide bi-directional power and communication flow to adjust the load and generation. Consequently, the cost is reduced, thus achieving one of the primary goals of the proposed work. Different strategies have been explored in the literature review for energy transactions with the MG and main grid within the MMG paradigm. The proposed work in this paper provides a realistic alternative to accomplish a solution concerning the technical, economical, and environmental concerns. Because each MG in the MMG paradigm retains RERs, the efficient energy management market controller (EEMMC) primarily transacts clean energy. For this reason, importing of energy from the primary grid is minimized and GHG emission is reduced likewise. The main grid is the least priority for transactive energy in the proposed work. The EEMMC asks each MG in the MMG about the status of energy and cost. Each MG GAC provides information according to the need of an hour or day. The provided information is secured with the EEMMC and is simultaneously shared by each MG. Depending upon the proposed model in this paper, the agent adopts a uniform clearing

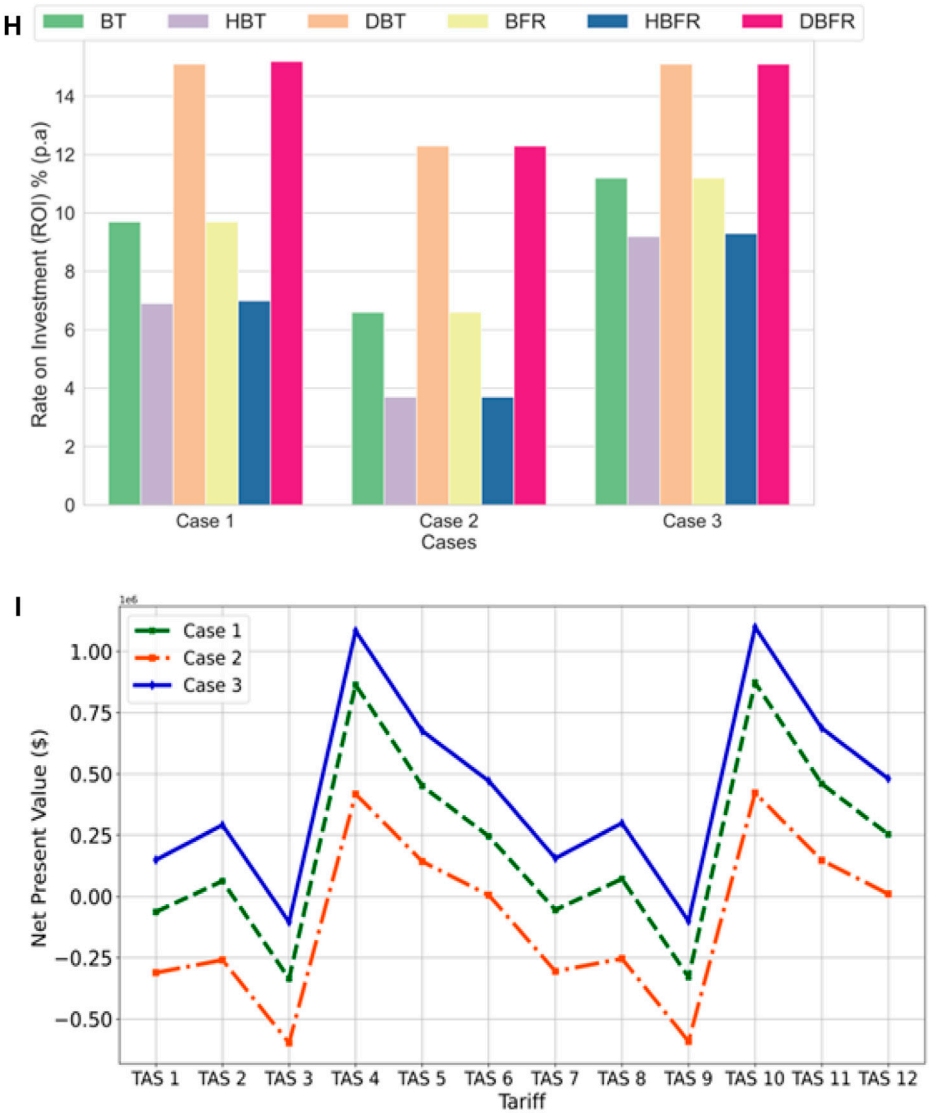

FIGURE 7
(Continued).

price and bilateral trading for real-time and day-ahead models in spot-market and future market environments, respectively. In the current project, a double-sided bidding method is being used to make the market more competitive. The proposed efficient energy market workflow is shown in Figure 4B.

3 Results and discussion

A proposed MMG paradigm in the current work incorporates residential, commercial, and industrial MGs. SRMGs comprise five rich-, seven middle-, and 12 poor-class homes, categorized on the basis of appliances. The SCMG is classified into large, medium, and small-scale commercial areas covering different appliances installed in commercial markets, educational institutes, hospitals, offices, and agricultural land. Cement and olive oil production are the sectors of the industrial grid that use high and medium energy levels, respectively. All the three MGs are integrated within an MAS environment through modern communication patterns. Two models, day-ahead and real-time models, are presented based on the time signal received. The model proposed in this paper is designed and programmed so that it tends to be effectively adopted according to each MG's needs and planning. The business-as-usual (BAU) load represents the consumer's unscheduled device usage or not optimized load pattern.

3.1 RTM for the MMG

3.1.1 RTM cases for SRMGs

The proposed model in the paper is built by considering different installed RER capacities, as given in Table 2, for SRMGs. Agents in the real-time model (RTM) receive hourly signals for the MMG paradigm's operation. In an uncertain environment, the agents perform an intelligent action to optimize the operation of each MG and accomplish the defined objectives. Figure 5A represents a base case of hourly operation of SRMGs.

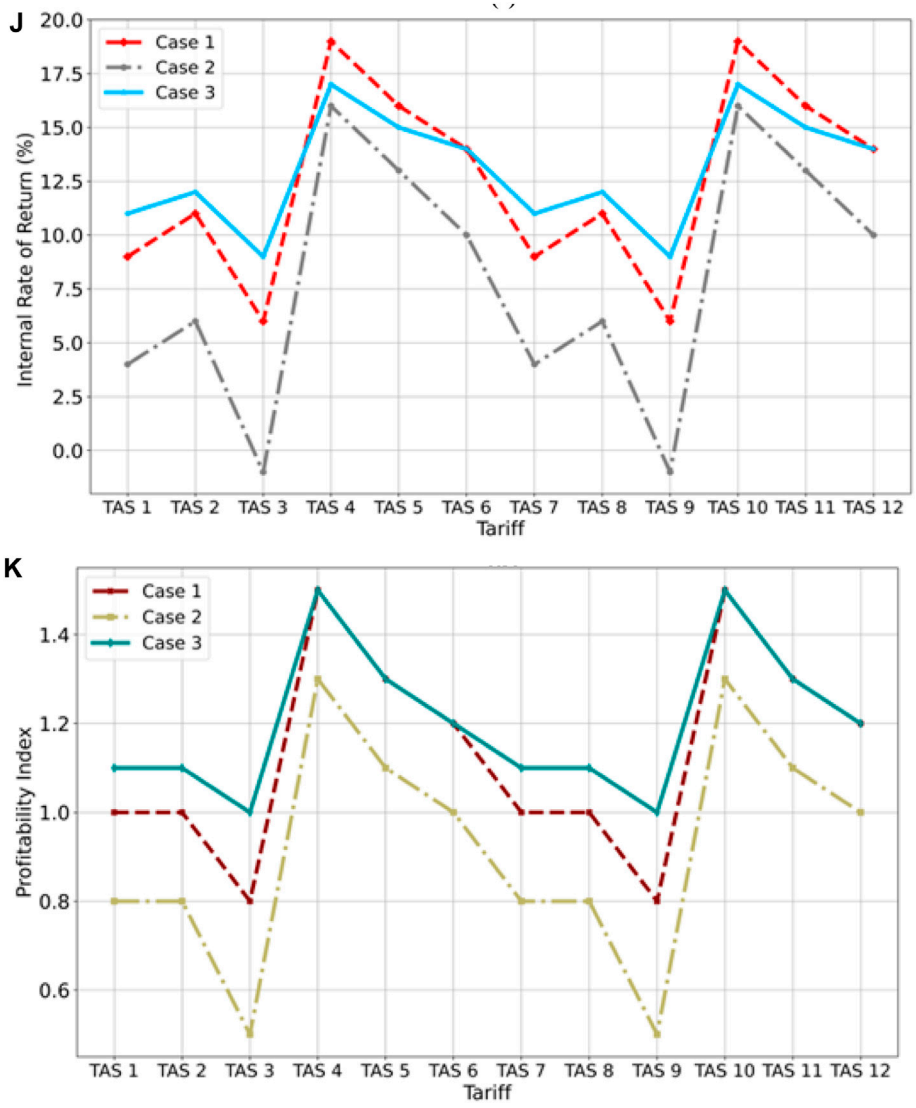

FIGURE 7
(Continued). Illustration of the RTM of SIMGs: **(A)** base case power flow; **(B)**, **(C)**, and **(D)** base case status of schedule devices; **(E)** case 1; **(F)** case 2; CBA of the proposed tariff; **(G)** PBP; **(H)** ROI; CBA of the proposed TAS; **(I)** NPV; **(J)** IRR; and **(K)** PI.

Figure 5A depicts that as the peak generation of the introduced RER is more prominent than the maximum load, the imported power by SRMGs is low in contrast to its exported power. The initial hours of power deficiency are satisfied by the BESS. Due to the non-availability of power in the energy market, power is imported from the main grid to satisfy the load demand at hours 19–23 by the bidding price mentioned in Table 2. Similarly, surplus power is exported to SCMGs at hour 5 and the main grid at hours 5–17 through the energy market, with offer price shown in Table 2. Furthermore, Figure 5A demonstrates the effective scheduling of the total load by MMPPnP considering the generation curve and incoming tariff as compared to the unscheduled BAU load. As shown in Figures 5B, C, the TFD and PFD agents turn ON/OFF devices at the ON-peak and OFF-peak hours of generation. The device status, ON and OFF, is represented by 0 and 1, respectively. Status 1 and status 2 for PFDs correspond to the minimum and maximum thermostat levels, respectively. The thermostat is set at the maximum level at ON-peak hours of generation, resulting in maximum user comfort with minimum cost. In contrast, the thermostat level is changed to status 1 at OFF-peak RER generation hours.

Figure 5D is the graphical representation of case 1 of SRMGs. Figure 5D depicts that RERs cannot meet the scheduled load demand during OFF-peak generation hours. As a result, initially, limited power is taken from batteries. Then, the SRMG approaches the energy market to meet the remaining load demand. Due to the volatile nature of the market, power import from the main grid is more than that of other MGs. Agents deployed in SRMGs intelligently optimize thermostat levels for PFDs at low generation hours. Due to the high installed capacity, as given in Table 2, the SRMG exports more energy in case 3, resulting in negligible energy import as compared to case 1 and case 2. Because of enough surplus power, as shown in Figure 5E, the thermostat of PFDs is positioned to a maximum level, reflecting the efficient

TABLE 6 Essential details of the MMG in the DAM.

MG	SRMG	SCMG	SIMG
Schedule load ($)	2,662.3	13,081.8	7,324.6
BAU load ($)	4,031.9	13,875.8	7,613.2
Emissions from RERs (g/kWh)	36,001	125,468	88,014
Emissions from the coal grid (g/kWh)	1,311,169	4,665,652	3,146,513
Decrease in emissions (%)	97.25427	97.31082	97.2028
Future contract settlement of SRMGs with SCMGs and SIMGs			
MGs	Industrial	Commercial	
Export (kW)	0	128.92934	
Import (kW)	24.1026172	0	
Export price ($/kWh)	0	0.08	
Import price ($/kWh)	0.095	0	
Future contract settlement of SCMGs with SRMGs and SIMGs			
Export (kW)	328.39056	127.5114364	
Import (kW)	440.9856713	99.12766626	
Export price ($/kWh)	0.09	0.08	
Import price ($/kWh)	0.095	0.075	
Future contract settlement of SIMGs with SRMGs and SCMGs			
Export (kW)	1,162.456364	312.3887344	
Import (kW)	0	0	
Export price ($/kWh)	0.095	0.09	
Import price ($/kWh)	0	0	

working of agents. The energy transactions for case 3 can be visualized in Figure 5E. Due to the unavailability of power in the market, the load demand from hours 21 to 23 is satisfied by the main grid. The monthly bill for the schedule load and BAU load pattern is calculated by considering the cost of the power taken from the RER, battery, and other MGs. It can be seen from Table 2 that the monthly bill for scheduled load is lower than that for the unscheduled load in all three cases of renewable power generation. This reflects the compelling and optimal load scheduling by deploying the proposed MMPPnP in RTM SRMGs. The increasing pattern of the schedule load cost in case 2 and case 3 shows the intelligent setting of the thermostat by agents for PFDs. Similarly, the decreasing trend of the BAU load shows the availability of more surplus power in subsequent cases.

At any hour, power is taken from RERs, batteries, and other renewable MGs (SCMGs and SIMGs) to meet the load demand by avoiding the grid, equivalent to reducing carbon emissions. Table 2 shows the emissions of SRMGs for the three cases of renewable energy generation. Table 2 depicts a tremendous decrease in carbon emissions if a load is satisfied from renewable sources compared to meeting the same. The cost–benefit analysis of SRMGs is determined by considering different parameters which are calculated to reference the investors or IPPs for implementing the proposed framework. The proposed tariff breakdown for the proposed model is given in Table 11. The Base TOU tariff is decided based on the solar FiT set for local residential areas in Pakistan. Half-base and double-base TOUs represent the half and double tariff of the base TOU, respectively. The base flat rate is the average sum of the base TOU ON and OFF-peak generation tariff.

As demonstrated in Figures 5A, F, the sensitivity analysis for the proposed model has determined the payback period for different cases. Figure 5F depicts that case 1 has a more extended payback period for different tariffs than cases 2 and 3. Due to the lowest tariff charge by the investor for selling power, as given in Table 3, the half-base TOU and half-base flat rate tariffs in each scenario have a more extended payback period. Because of the significant investment and low demand fulfillment from RERs, these two tariffs are considered invalid for case 1. On the contrary, double-base TOU and double-base flat rate tariffs exhibit the best results for selecting tariffs in each case. The best outcome for all the instances is provided by case 3, which has a short payback period for all tariffs. This results from RER electricity being used to its fullest potential to meet the load demand.

The annual return-on-investment for each of the three RTM SRMG cases is shown in Figure 5G. The ROI for half-base TOU

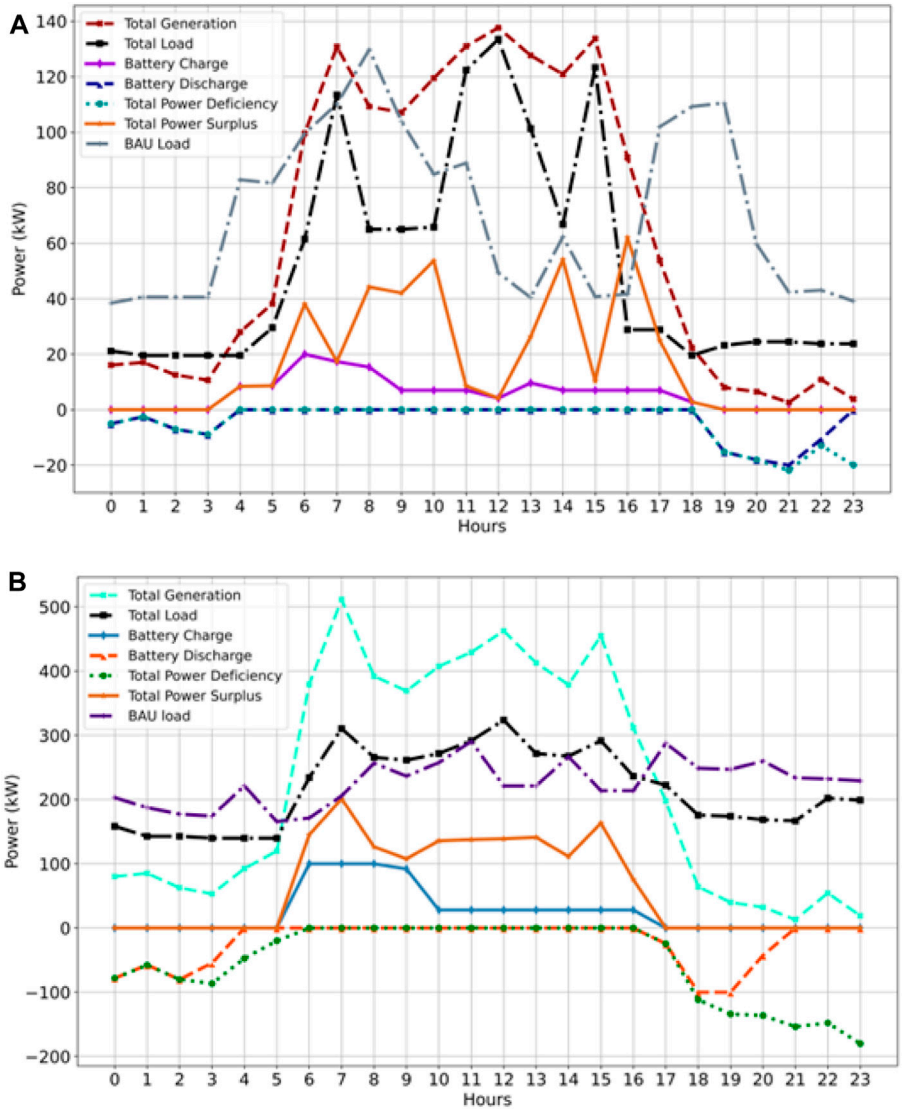

FIGURE 8
(Continued).

and half-base flat rate tariff, observed in Figure 5G, is considered to be the lowest in all cases. In contrast, double-base TOU and the double-base flat rate have the highest ROI values for different capacities of RERs. Case 1 in Figure 5G is assessed as infeasible for the investors as it has the lowest ROI. This is due to the increase in power import from other MGs and the main grid to meet the demand. On the other hand, case 3 is considered the most feasible as it has the highest values of ROIs for different tariffs. The current work proposes different tariff adjustment strategies given in Table 3 to calculate the NPV, PI, and IRR for different installed capacities of RERs. Figure 5H illustrates the NPV of SRMGs by adopting various tariff adjustment strategies (TASs) for different cases. It can be seen in Figure 5H that TAS 3 and TAS 9 have the lowest NPV, but TAS 10 has the best NPV among all situations. Additionally, as seen in Figure 5I, IRR is kept to a minimum by adhering to TAS 3 and 9. The adoption of TAS 4, however, results in the greatest IRR. The highest and lowest IRRs between these cases can be seen in case 1. Case 2 has the highest PI through implementing TAS 10, as shown in Figure 5J. However, RER installation, as in case 1, is infeasible to pursue as its PI is less than 1 in most TASs.

3.1.2 RTM cases for SCMGs

The RTM of SCMGs is evaluated through an acquaintance of different scenarios and their economic assessment. Therefore, the load demand is maintained throughout. Different cases are taken into consideration based on the capacity of the installed RER, as represented in Table 4. RERs with 1000 kW capacity are installed for the base case of SCMGs. It can be seen from the graphical representation of SCMGs, in Figure 6A, that power export is maximum at the ON-peak hour of generation. In contrast, power is initially imported from the battery and then the SCMG

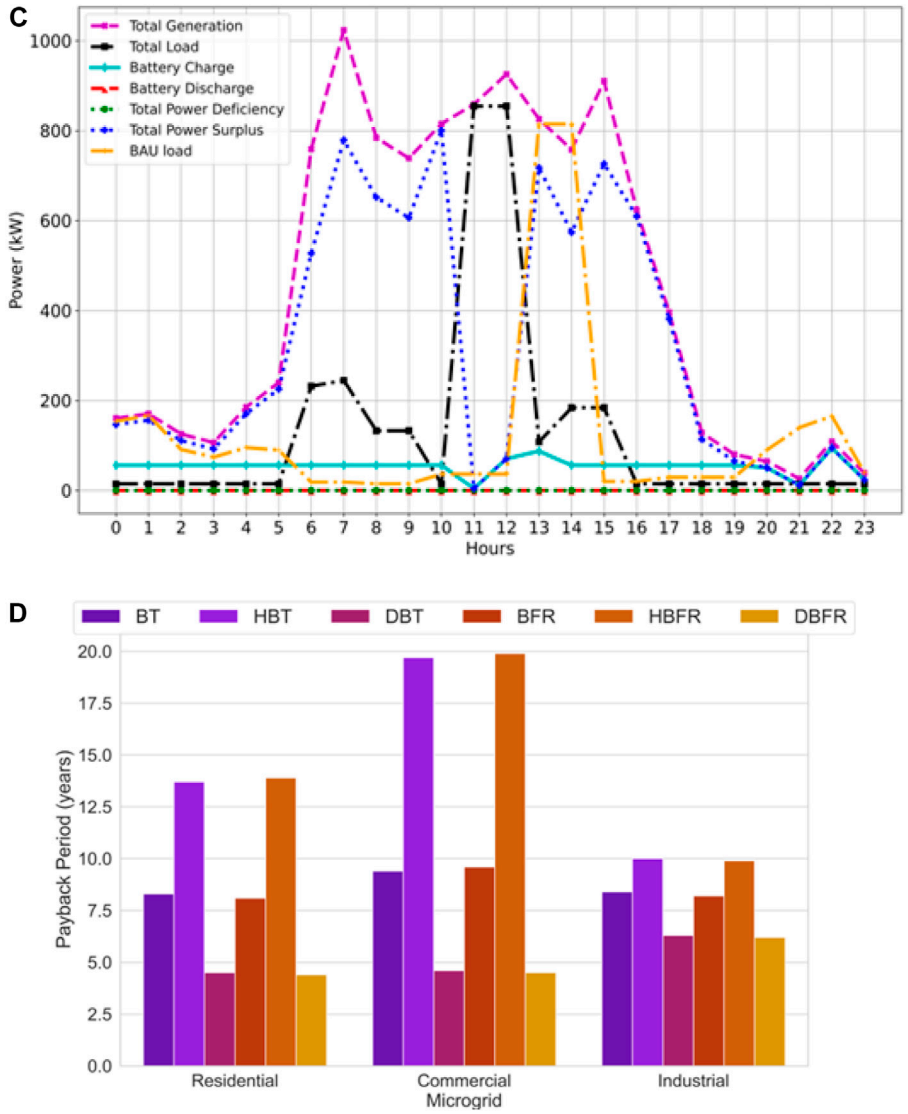

FIGURE 8
(Continued).

approaches to the energy for meeting the scheduled load. At power deficit hours 3, 4, 5, 18, and 19, power is imported from SRMGs and SIMGs by bidding the price given in Table 4. The corresponding signal is communicated to the efficient energy market in the RTM for every hour with excess or lack of power. The SCMG places an offer and bid for the corresponding power through the communicated signal.

Figure 6E demonstrates that the load curve is more dominant than the generation curve at off-peak hours for case 1. As a result, initially, limited power is taken from batteries. Then, SCMGs approach the energy market to meet the remaining load demand. As shown in Figure 6E, deficiency is satisfied by taking power from the SIMG at hours 3, 4, 5, 18, and 19. Similarly, the SRMG provides energy to the SCMG at hour 5, but the market clears at an industrial bid. Thus, the SRMG experiences social welfare benefit from the market environment. Power is taken from the main grid at 3, 4, 18, 19, 20, 21, 22, and 23 h due to insufficient power to satisfy the load. Due to the volatile nature of the market, power import from the main grid is more than that of the other MGs.

Case 3 consists of RERs with the highest capacity as provided in Figure 6F. Consequently, the thermostat is tuned to a maximum level and maximum energy is exported to other MGs as compared to other cases. Consequently, less electricity is purchased from the energy market than in the other scenarios. At load surplus hours of 9, 11, 12, 13, and 14, power is exported to SIMGs and SRMGs at the offer price shown in Table 4. The cost of the electricity used from RERs, batteries, and other MGs is considered while calculating the monthly bill for the schedule load and the BAU load. Scheduled load cost in case 3 is the lowest, as shown in Table 4. This is due to the minimum power import from other MGs and the maximum utilization of clean energy. The low cost of the schedule load shows the efficient and effective load scheduling achieved by implementing the suggested

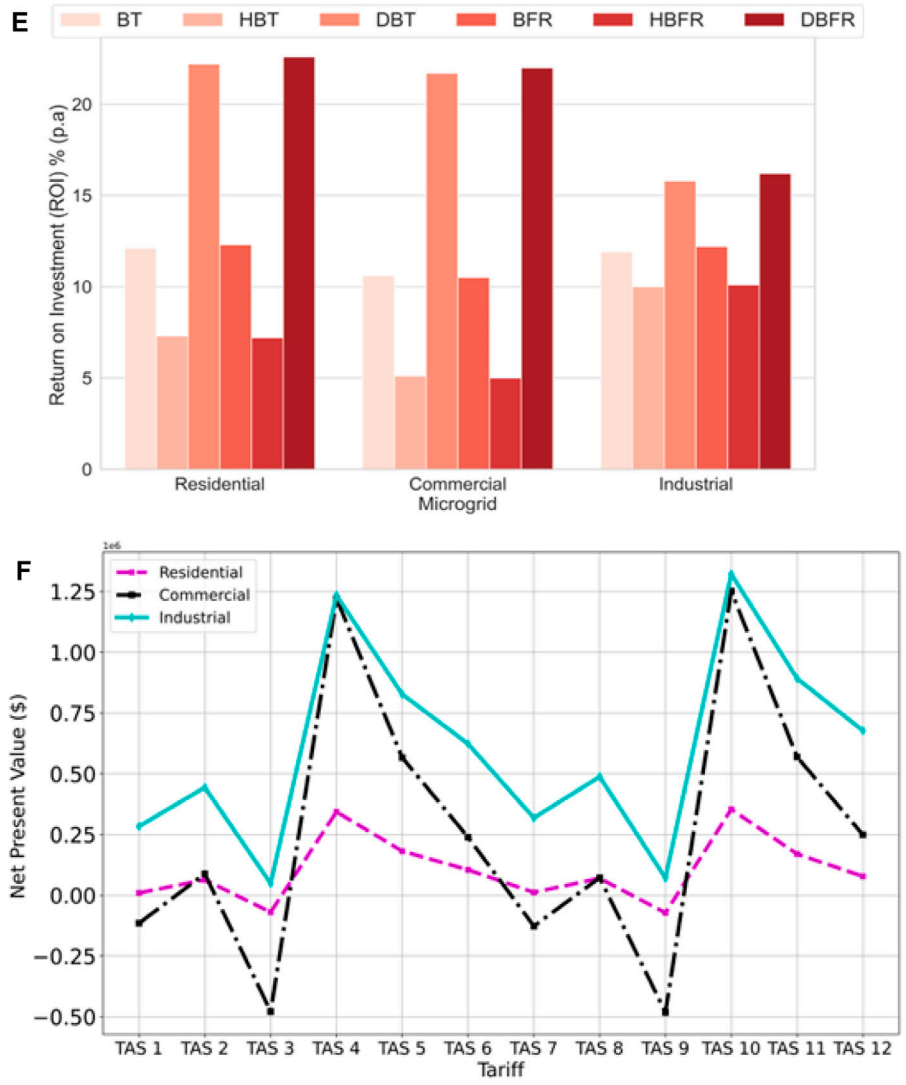

FIGURE 8
(Continued).

MMPPnP and knapsack in RTM SCMGs. Carbon dioxide emission by taking power from the main grid is minimized by importing power from RERs, batteries, and other MGs with RERs. Emissions from SCMGs satiating the same demand from the main grid and RERs are demonstrated in Table 4. It can be seen from Table 4 that there is a prominent decrease in emissions that can be achieved through the proposed work.

For executing the proposed framework for SCMGs, specific metrics of CBA are calculated to pave the way for investors or IPPs. Three scenarios are put into consideration based on the capacity of the installed RER. As shown in Figure 6G, the suggested model's sensitivity analysis was used to evaluate the payback period for the defined cases. It can be analyzed from Figure 6G that there is a prominent decrease in PB for different cases by adopting half-base TOU and the half-base flat rate tariff. Furthermore, by introducing additional tariffs, PB also reduces the ascendingly arranged cases. The primary factor behind the decline in PB is the maximum use of clean energy. However, the capital and operating costs of a large number of RERs cause the PB of the installed setup to be delayed, even though clean energy usage is constant. Case 1 in Figure 6H has the lowest and highest ROI by deploying half-base TOU, half-base flat rate, double-base TOU, and double-base flat rate tariffs, respectively. This is because of the low initial and operation costs and maximum utilization of clean energy. It can be seen from Figure 6I that adopting TAS 4 and TAS 10, given in Table 4, achieves the highest NPV for SCMGs. Moreover, case 1 has the highest IRR for TAS 4 and TAS 10, as demonstrated in Figure 6J. The PI for different cases by deploying various TASs is illustrated in Figure 6K. The analysis in Figure 6K reveals that case 1 achieved the highest PI by using TAS 4 and TAS 10 in the RTM for SCMGs.

3.1.3 RTM cases for SIMGs

Table 5 shows the values of installed RERs, which are taken into consideration for the evaluation of different cases of the RTM for

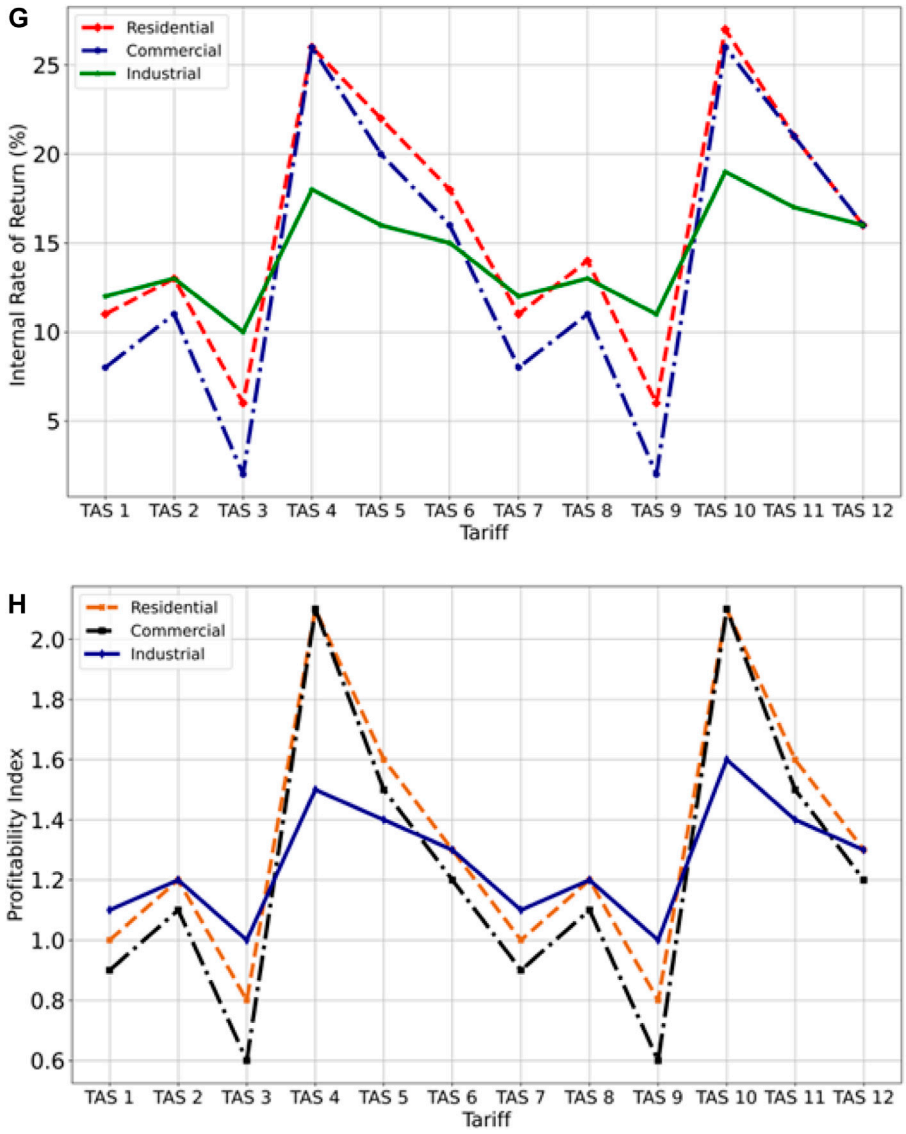

FIGURE 8
(Continued). Power flow of the DAM base case of **(A)** the SRMG; **(B)** SIMG; **(C)** SCMG, CBA of the proposed tariff for MMGs; **(D)** PBP; **(E)** ROI, CBA of the proposed TAS for MMGs; **(F)** NPV; **(G)** IRR; and **(H)** PI.

SIMGs. The capacity of the installed RER for case 3 is the highest among other cases. Due to the highest capacity of the installed RER in SIMGs, the generation curve is highly dominant along 24 h, as shown in Figure 7A. Consequently, the SIMG experiences no power deficiency as the total scheduled load demand is met by the installed RER. Due to high surplus power, the maximum power is exported to nearby MGs and the main grid by offering it in the energy market at the price given in Table 5. Figure 7 (B–D) shows the optimal scheduling of devices in SIMGs by deploying MMPPnP.

The energy flow in SIMGs for case 1 by deploying the RTM is represented in Figure 7E. It can be seen from Figure 7E that most of the load is satisfied by clean energy, and the remaining surplus power is communicated to the energy market for trading. However, at hours 11 and 12, the SIMG approaches SCMGs to satisfy the scheduled load. Further power deficiency is satisfied by the main grid at a high tariff. Case 2 has the lowest capacity for the installed RER and is illustrated in Figure 7F. Due to the low power provided by RERs at hours 11 and 12, the SIMG approaches the energy market where the SCMG is the only provider of energy. As a result, the SIMG imports power from the SCMG at a low price by avoiding the high price main-grid energy import, as given in Table 5. The monthly bill of the scheduled and BAU load for SIMGs is provided in Table 5. Case 2 has the lowest monthly bill due to the low price of power import from the SCMG and SIMG. While in other cases, the low power is satisfied by importing power from the main grid mostly. Furthermore, PFDs in the SIMG operate at a low-rated power at hours of low generation. Consequently, the PFD in case 3 operates at the maximum rated power and increases the bill cost.

By importing energy from RERs, batteries, and other MGs with RERs, carbon dioxide emissions caused by using the power from the main grid are reduced to a minimum. Table 5 shows emissions from

the SIMG satisfying the same demand from the main grid and RERs. As given in Table 5, the proposed work has the potential to reduce emissions significantly. Specific CBA parameters are estimated based on the capacities of the installed RERs to provide an idea for investors or IPPs in executing the suggested framework for SIMGs. Different CBA parameters are calculated for the proposed tariff given in Table 5.

The payback period for different cases of the SIMG is illustrated in Figure 7G. It can be seen from Figure 7G that case 3 has the shortest PB. This is due to the maximum utilization of RERs by the SIMG and low power import. Consequently, ROIs for different tariffs of case 3 are maximum compared to other cases shown in Figure 7H. The NPV for the RTM SIMG, given in Figure 7I, shows that case 3 shows a dominant difference among different cases for various TASs suggested in Table 5. Figure 7J shows that case 1 has a high IRR compared to case 3 by adopting TAS 4 and 10. However, case 3 gives a high IRR for the rest of TASs. As seen in Figure 7K, case 3 is the most feasible, whereas case 2 is the least feasible to pursue for different TASs.

3.2 Day-ahead model for the MMG paradigm

The DAM's operation is based upon the forecasted data where DA signals are communicated only once to the agents at the start of each day. The monthly bill for the base case of the DAM in the MMG paradigm is calculated and is given in Table 6, i.e., MMGWO for the DAM efficiently minimizes the cost of load consumption by effective scheduling of the load as compared to the BAU. Deployed intelligent agents efficiently optimize the signals and plans intelligently for achieving defined objectives. Figure 8A visualizes the energy flow operation by deploying the DAM in the SRMG, and it is observed that the maximum load is scheduled at signal hours of low tariff and maximum renewable energy generation. At hours of maximum surplus, the battery is charged first, and then the remaining surplus power is sent to the market for energy transactions. Furthermore, Figures 8B, C show the power flow of SCMGs and SIMGs over 24 h, respectively. During hours 5–17, the RER generation is greater than the load scheduled, and the thermostat is adjusted to a maximum level, and maximum number of devices are turned ON to minimize the cost and maximize the UC. The comparative analysis of proposed tariffs and their adjustments are shown in Figures 8D–E and Figures 8F–H, respectively.

4 Conclusion

The proposed work develops an intelligent and efficient MAS framework in three different load-based MGs in the MMG paradigm. An adequate communication infrastructure among agents is implemented to complete the distributed tasks smartly. The proposed work aims to maximize RER utilization, reduce monthly consumer bill, maximize user-comfort, and reduce emissions. MMPPnP, MMGWO, and knapsack are deployed concurrently with the demand dispatch and demand response techniques for real-time and day-ahead signals to obtain optimum results for the defined objectives. Intelligent thermostat agents set the optimal temperature of the HVAC and AC according to the ASHRAE standard 55-2010 depending upon the incoming P_{sur} signal. An efficient energy market is developed to provide spot-market and future market environments for real-time and day-ahead signals, respectively. The current work offers future prospects for the IPPs or investors by introducing different tariff adjustment techniques, which provides a win–win situation for the investor and consumer. Each MG is evaluated on the basis of the capacity of the installed RERs and its effect on emissions, monthly bill reduction, cost–benefit analysis, and energy transactions for both real-time and day-ahead signals. Considering a base case for the deployed RTM for each MG as case 2, the capacity of the installed RER is increased and decreased in case 1 and case 3, respectively. The results show that case 1 of SRMGs and SCMGs, whereas case 2 of SIMGs has the lowest CO_2 emissions as 97.6083%, 97.6359%, and 97.3084%, respectively. Case 2 of SRMGs and SCMGs has the lowest monthly bill among other cases. Similarly, the monthly bill is low for case 3 as compared to that of case 1 and case 2 in SIMGs. Different TASs are proposed for the investors to deploy. Case 3 shows the best results in terms of the PB, ROI, and NPV, whereas the IRR and PI are the highest for case 1 and case 2 in SRMGs. For SCMGs, PB and NPV are the lowest and highest for case 3 in commercial MGs, respectively. Additionally, case 1 shows the highest values for the IRR, PI, and ROI, whereas case 3 has the best average value for the ROI in the commercial MG. Furthermore, case 3 of SIMGs has the best values for the PB, ROI, PI, and NPV, but case 1 achieves the highest IRR. Future market cases show that under the considered scenarios, SIMGs have the lowest PB and highest NPV. Furthermore, SRMGs have the highest ROI, PI, and IRR for settling future contracts. The optimized results based upon the cost–benefit analysis, cost reduction, power transaction in the market, and maximum utilization of RERs have been obtained for each MG. In the future, hardware implementation for the current work will be carried out by providing a secure environment for the power and payment methodology.

Data availability statement

The original contributions presented in the study are included in the article/Supplementary Material; further inquiries can be directed to the corresponding authors.

Author contributions

KM: formal analysis, investigation, software, and writing–original draft. AA: funding acquisition, methodology, resources, supervision, validation, and writing–original draft. SK: conceptualization, formal analysis, methodology, resources, and writing–original draft. ZK: conceptualization, data curation, formal analysis, funding acquisition, supervision, and writing–review and editing. BA: investigation, project administration, software, validation, visualization, and

writing–review and editing. HAla: investigation, project administration, resources, validation, visualization, and writing–review and editing. HAls: data curation, project administration, resources, visualization, and writing–review and editing. AM: data curation, funding acquisition, methodology, and writing–review and editing.

Funding

The author(s) declare that financial support was received for the research, authorship, and/or publication of this article. The authors extend their appreciation to the Deputyship for Research and Innovation, Ministry Education in Saudi Arabia, for funding this research work through the project number (IFP-2022-44).

Conflict of interest

The authors declare that the research was conducted in the absence of any commercial or financial relationships that could be construed as a potential conflict of interest.

Publisher's note

References

Ahmadi, S. E., and Rezaei, N. (2020). A new isolated renewable based multi microgrid optimal energy management system considering uncertainty and demand response. *Int. J. Electr. Power and Energy Syst.* 118, 105760. doi:10.1016/j.ijepes.2019.105760

Alam, M. N., Chakrabarti, S., and Liang, X. (2020). A benchmark test system for networked microgrids. *IEEE Trans. Ind. Inf.* 16 (10), 6217–6230. doi:10.1109/tii.2020.2976893

Ali, S. A., Hussain, A., Haider, W., Rehman, H. U., and Kazmi, S. A. A. (2023). Optimal energy management system of isolated multi-microgrids with local energy transactive market with indigenous PV-Wind-and biomass-based resources. *Energies (Basel)* 16, 1667. doi:10.3390/en16041667

Bui, V., Member, S., Hussain, A., and Member, S. (2018). A multiagent-based hierarchical energy management strategy for multi-microgrids considering adjustable power and demand response. *IEEE Trans. Smart Grid* 9 (2), 1323–1333. doi:10.1109/tsg.2016.2585671

Choobineh, M., and Mohagheghi, S. (2016). A multi-objective optimization framework for energy and asset management in an industrial Microgrid. *J. Clean. Prod.* 139, 1326–1338. doi:10.1016/j.jclepro.2016.08.138

Cortes, C. A., Contreras, S. F., and Shahidehpour, M. (2017). Microgrid topology planning for enhancing the reliability of active distribution networks. *IEEE Trans. Smart Grid* 9 (6), 6369–6377. doi:10.1109/tsg.2017.2709699

Dong, X., Li, X., and Cheng, S. (2020). Energy management optimization of microgrid cluster based on multi-agent-system and hierarchical stackelberg game theory. *IEEE Access* 8, 206183–206197. doi:10.1109/ACCESS.2020.3037676

Guo, Z., Pinson, P., Chen, S., Yang, Q., and Yang, Z. (2021). Online optimization for real-time peer-to-peer electricity market mechanisms. *IEEE Trans. Smart Grid* 12 (5), 4151–4163. doi:10.1109/tsg.2021.3075707

Hannan, M. A., Lipu, M. S. H., Hussain, A., and Mohamed, A. (2017). A review of lithium-ion battery state of charge estimation and management system in electric vehicle applications: challenges and recommendations. *Renew. Sustain. Energy Rev.* 78, 834–854. doi:10.1016/j.rser.2017.05.001

Haseeb, M., Kazmi, S. A. A., Malik, M. M., Ali, S., Bukhari, S. B., and Shin, D. R. (2020). Multi objective based framework for energy management of smart micro-grid. *IEEE Access* 8, 220302–220319. doi:10.1109/ACCESS.2020.3041473

Hirsch, A., Parag, Y., and Guerrero, J. (2018). Microgrids: a review of technologies, key drivers, and outstanding issues. *Renew. Sustain. Energy Rev.* 90, 402–411. doi:10.1016/j.rser.2018.03.040

Husein, M., and Chung, I.-Y. (2018). Optimal design and financial feasibility of a university campus microgrid considering renewable energy incentives. *Appl. Energy* 225, 273–289. doi:10.1016/j.apenergy.2018.05.036

IEA (2020). Global Energy Review 2019 - the latest trends in energy and emissions in 2019. *Glob. Energy Trends*, 1–50.

Karimi, H., Gharehpetian, G. B., Ahmadiahangar, R., and Rosin, A. (2023). Optimal energy management of grid-connected multi-microgrid systems considering demand-side flexibility: a two-stage multi-objective approach. *Electr. Power Syst. Res.* 214, 108902. doi:10.1016/j.epsr.2022.108902

Karimi, H., and Jadid, S. (2023). Multi-layer energy management of smart integrated-energy microgrid systems considering generation and demand-side flexibility. *Appl. Energy* 339 (Jun), 120984–122023. doi:10.1016/j.apenergy.2023.120984

Khalid, R., Javaid, N., Rahim, M. H., Aslam, S., and Sher, A. (2019). Fuzzy energy management controller and scheduler for smart homes. *Sustain. Comput. Inf. Syst.* 21, 103–118. doi:10.1016/j.suscom.2018.11.010

Liang, Z., Bian, D., Zhang, X., Shi, D., Diao, R., and Wang, Z. (2019). Optimal energy management for commercial buildings considering comprehensive comfort levels in a retail electricity market. *Appl. Energy* 236, 916–926. doi:10.1016/j.apenergy.2018.12.048

Liu, Y., Wang, Y., Li, Y., Gooi, H., and Xin, H. (2021). Multi-agent based optimal scheduling and trading for multi-microgrids integrated with urban transportation networks. *IEEE Trans. Power Syst.* 36 (3), 2197–2210. doi:10.1109/tpwrs.2020.3040310

Malik, M. M., Kazmi, S. A. A., Asim, H. W., bin Ahmed, A., and Shin, D. R. (2020). An intelligent multi-stage optimization approach for community based micro-grid within multi-microgrid paradigm. *IEEE Access* 8, 177228–177244. doi:10.1109/ACCESS.2020.3022411

Mirjalili, S., Saremi, S., Mirjalili, S. M., and Coelho, L. dos S. (2016). Multi-objective grey wolf optimizer: a novel algorithm for multi-criterion optimization. *Expert Syst. Appl.* 47, 106–119. doi:10.1016/j.eswa.2015.10.039

Naderi, M., Bahramara, S., Khayat, Y., and Bevrani, H. (2017). Optimal planning in a developing industrial microgrid with sensitive loads. *Energy Rep.* 3, 124–134. doi:10.1016/j.egyr.2017.08.004

Oueid, R. K. (2019). Microgrid finance, revenue, and regulation considerations. *Electr. J.* 32 (5), 2–9. doi:10.1016/j.tej.2019.05.006

Purage, L., Isuru, M., Paudel, A., Nguyen, H. D., and Foo, E. Y. S. (2022). Peer-to-Peer energy trading enabled optimal decentralized operation of smart distribution grids. *IEEE Trans. Smart Grid* 13 (1), 654–666. doi:10.1109/TSG.2021.3110889

Rajaei, A., Fattaheian-dehkordi, S., Fotuhi-firuzabad, M., and Moeini-Aghtaie, M. (2020). Decentralized transactive energy management of multi-microgrid distribution systems based on ADMM," *Int. J. Electr. Power Energy Syst.* 132, 107126. doi:10.1016/j.ijepes.2021.107126

Ramadan, M., Mohamad, B., Logenthiran, T., Naayagi, R. T., and Woo, W. L. (2019). A nano-biased energy management using reinforced learning multi-agent on layered coalition model: consumer sovereignty. *IEEE Access* 7, 52542–52564. doi:10.1109/ACCESS.2019.2911543

Rezaei, N., Pezhmani, Y., and Khazali, A. (2022). Economic-environmental risk-averse optimal heat and power energy management of a grid-connected multi microgrid system considering demand response and bidding strategy. *Energy* 240, 122844. doi:10.1016/j.energy.2021.122844

Shi, S., Wang, Y., and Jin, J. (2023). Multi-agent-based control strategy for centerless energy management in microgrid clusters. *Front. Energy Res.* 11, 2023. doi:10.3389/fenrg.2023.1119461

Systems, M., Bazmohammadi, N., Anvari-moghaddam, A., Tahsiri, A., Vasquez, J., and Guerrero, J. (2020). Stochastic predictive energy management of multi-microgrid systems. *Appl. Sci. Stoch. Predict. Energy Manag.*10, 4833. doi:10.3390/app10144833

Tan, B., and Chen, H. (2020). Multi-objective energy management of multiple microgrids under random electric vehicle charging. *Energy* 208, 118360. doi:10.1016/j.energy.2020.118360

Thirugnanam, K., Moursi, M. S. E., Khadkikar, V., Zeineldin, H. H., and Al Hosani, M. (2021). Energy management of grid interconnected multi-microgrids based on P2P energy exchange: a data driven approach. *A Data Driven Approach* 36 (2), 1546–1562. doi:10.1109/TPWRS.2020.3025113

Ton, D. T., and Smith, M. A. (2012). The US department of energy's microgrid initiative. *Electr. J.* 25 (8), 84–94. doi:10.1016/j.tej.2012.09.013

Vu, B. H., Husein, M., Kang, H.-K., and Chung, I.-Y. (2019). Optimal design for a campus microgrid considering ESS discharging incentive and financial feasibility. *J. Electr. Eng. Technol.* 14 (3), 1095–1107. doi:10.1007/s42835-019-00142-9

Wang, S., Zhang, X., Wu, L., and Sun, S. (2018). New metrics for assessing the performance of multi-microgrid systems in stand-alone mode. *Int. J. Electr. Power and Energy Syst.* 98, 382–388. doi:10.1016/j.ijepes.2017.12.002

Xu, D., Zhong, F., and Bai, Z. (2023). A two-layer multi-energy management system for microgrids with solar, wind, and geothermal renewable energy. *Front. Energy Res.* 10 (Jan). doi:10.3389/fenrg.2022.1030662

Xu, Z., Yang, P., Zheng, C., Zhang, Y., Peng, J., and Zeng, Z. (2018). Analysis on the organization and Development of multi-microgrids. *Renew. Sustain. energy Rev.* 81, 2204–2216. doi:10.1016/j.rser.2017.06.032

Yang, X., He, H., Zhang, Y., Chen, Y., and Weng, G. (2019). Interactive energy management for enhancing power balances in multi-microgrids. *IEEE Trans. Smart Grid* 10 (6), 6055–6069. doi:10.1109/TSG.2019.2896182

Yin, L., and Li, S. (2021). Hybrid metaheuristic multi-layer reinforcement learning approach for two-level energy management strategy framework of multi-microgrid systems. *Eng. Appl. Artif. Intell.* 104, 104326. doi:10.1016/j.engappai.2021.104326

Zhong, X., Zhong, W., Liu, Y., Yang, C., and Xie, S. (2022). Optimal energy management for multi-energy multi-microgrid networks considering carbon emission limitations. *Energy* 246, 123428. doi:10.1016/j.energy.2022.123428

Zhuo, Z., Yang, K., Yang, J., Mao, R., and Xue, N. (2019). A multiagent-based hierarchical energy management strategy for maximization of renewable energy consumption in interconnected multi-microgrids. *IEEE Access* 7, 169931–169945. doi:10.1109/ACCESS.2019.2955552

Zlatkovic, M., Zlatkovic, S., Sullivan, T., Bjornstad, J., and Shahandashti, S. K. F. (2019). Assessment of effects of street connectivity on traffic performance and sustainability within communities and neighborhoods through traffic simulation. *Sustain Cities Soc.* 46, 101409. doi:10.1016/j.scs.2018.12.037